Cap. 15
Evolução de estrelas massivas

Desde **The Light Curves and the Radioactive Decay of the Ejecta**

AGA293

Jorge Meléndez

Estrutura de estrela massiva ($Massa_{inicial} > 9\ M_{Sol}$) antes do colapso do núcleo e explosão supernova

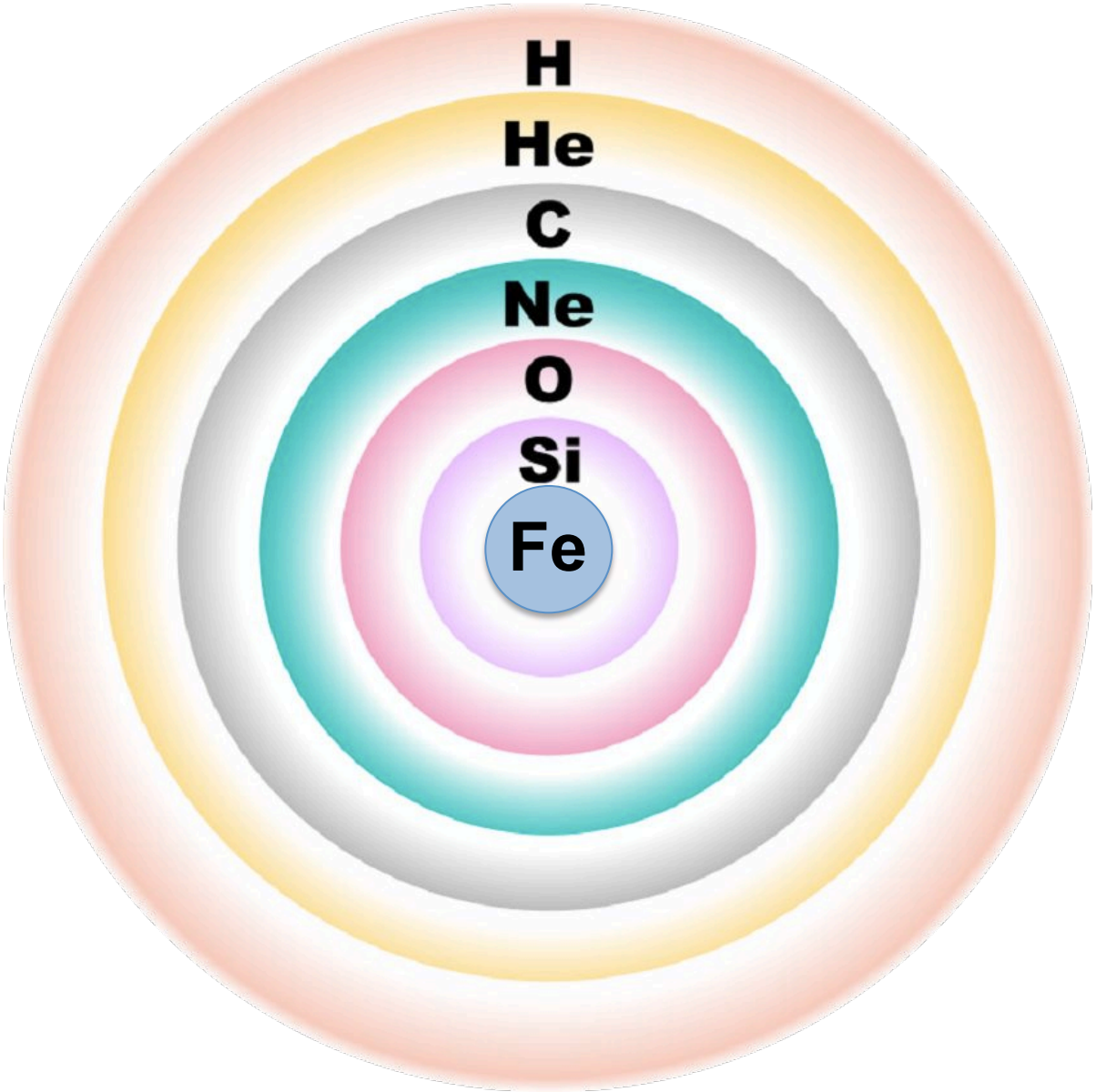

Estrutura pre-colapso de estrela massiva (massa inicial = 25 M_{Sol})

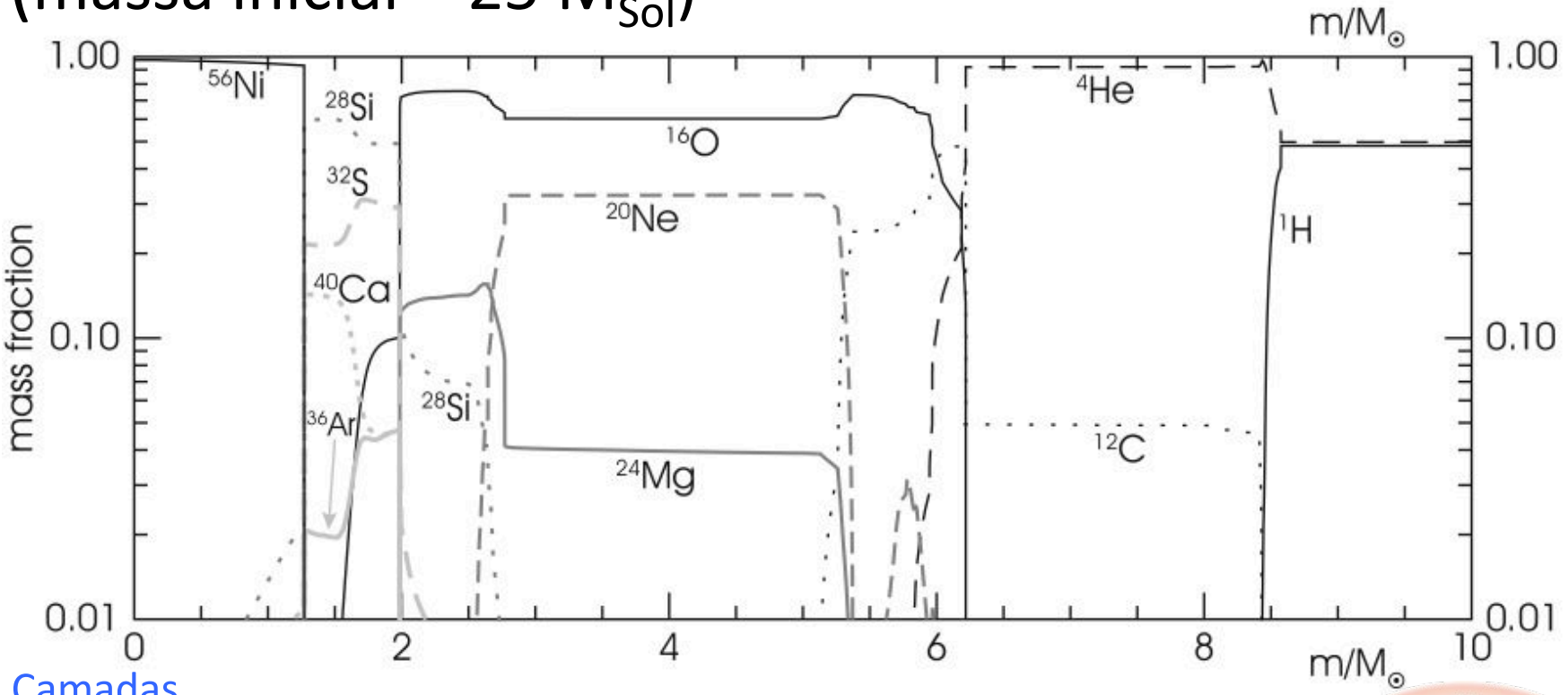

Camadas de queima

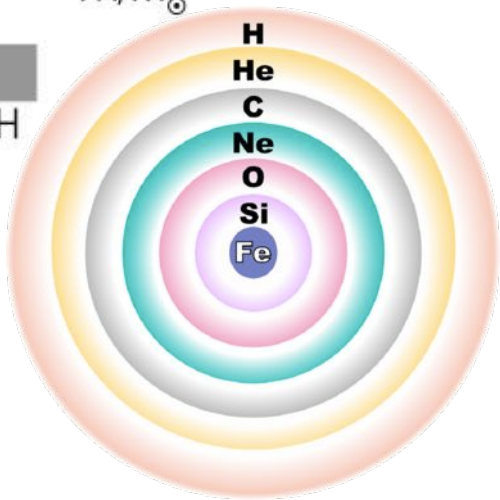

Fig. 36.4 The chemical composition in the interior of a highly evolved model of a population I star with an initial mass of $25M_{\odot}$, close to the end of hydrostatic nuclear burning. The mass at this time is reduced to $16M_{\odot}$ due to mass loss. In the *upper panel* the mass concentrations of important elements are plotted against the mass variable m. *Below* the abscissa, in the *middle* of the figure, the approximate location of shell sources in different nuclear burning phases is indicated by the *grey rectangles*.

Kippenhahn et al. 2012: Stellar Structure & Evolution, 2nd Ed.

Estrutura pre-colapso de estrela massiva (massa inicial > 9 M_{Sol})

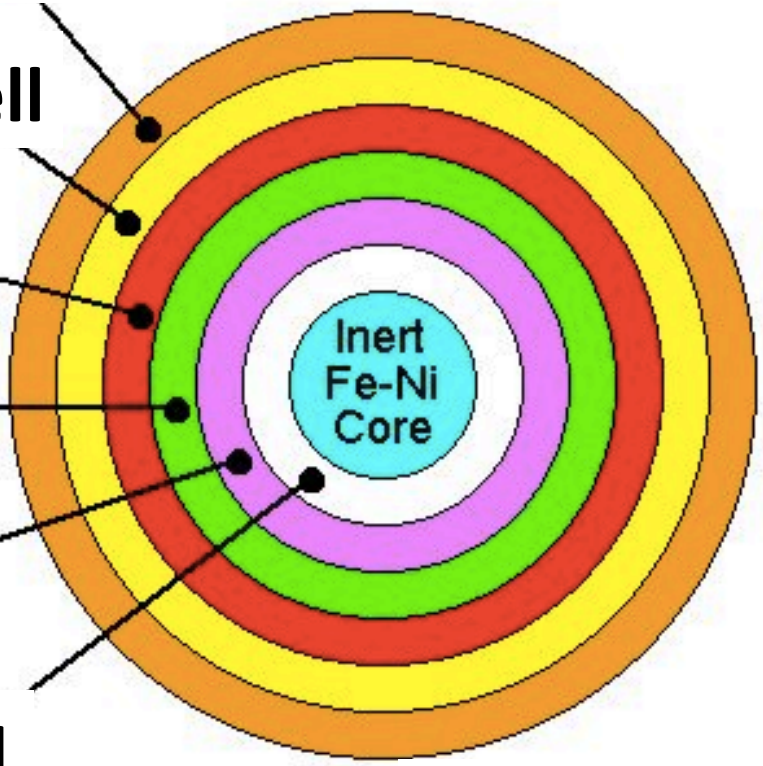

http://www.astronomy.ohio-state.edu/~pogge/Ast162/Unit3/supernova.html

Estrutura pre-colapso de estrela massiva

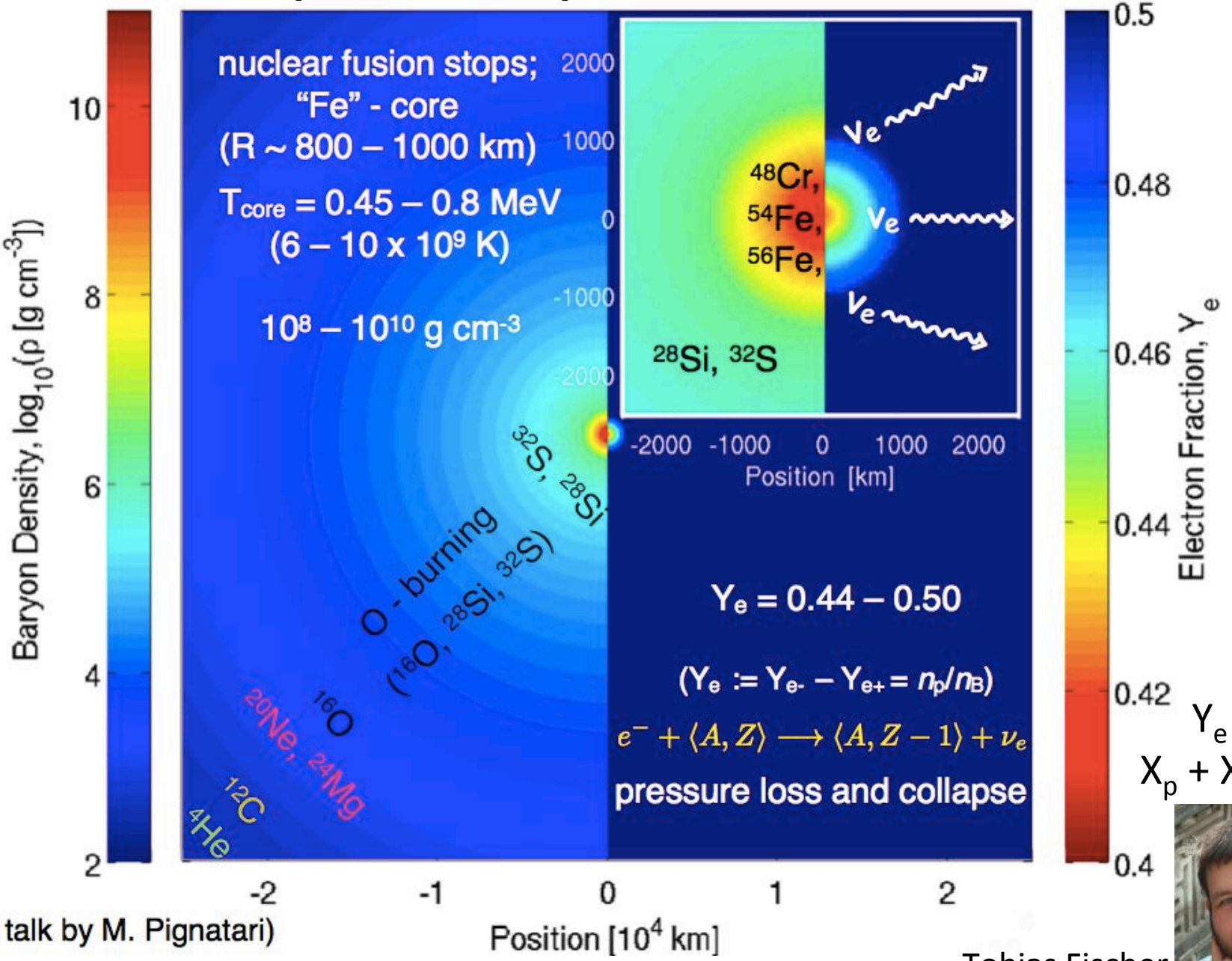

(see talk by M. Pignatari)

$Y_e = X_p$

$X_p + X_p = 1$

Tobias Fischer

Nucleossíntese no rebote

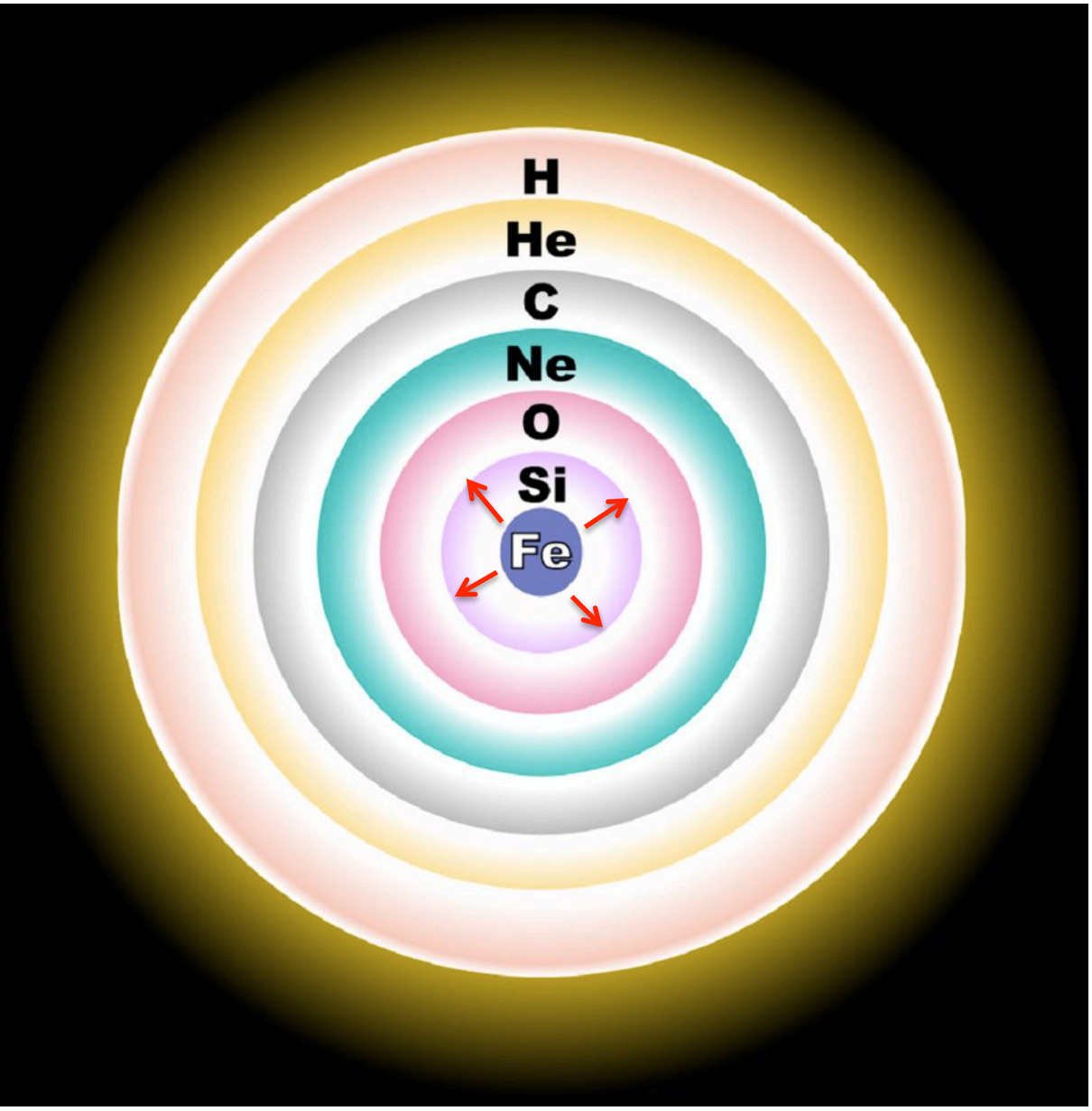

$^{28}_{14}Si + {}^{4}_{2}He \rightarrow {}^{32}_{16}S$

$^{32}_{16}S + {}^{4}_{2}He \rightarrow {}^{36}_{18}Ar$

$^{36}_{18}Ar + {}^{4}_{2}He \rightarrow {}^{40}_{20}Ca$

$^{40}_{20}Ca + {}^{4}_{2}He \rightarrow {}^{44}_{22}Ti$

$^{44}_{22}Ti + {}^{4}_{2}He \rightarrow {}^{48}_{24}Cr$

$^{48}_{24}Cr + {}^{4}_{2}He \rightarrow {}^{52}_{26}Fe$

$^{52}_{26}Fe + {}^{4}_{2}He \rightarrow {}^{56}_{28}Ni$

$^{56}_{28}Ni + {}^{4}_{2}He \rightarrow {}^{60}_{30}Zn$

E outras reações, por ex. :

$^{52}_{24}Cr + {}^{4}_{2}He \rightarrow {}^{56}_{26}Fe$

As supernovas mais comuns de colapso de núcleo são as tipo II-P (*Plateau*)

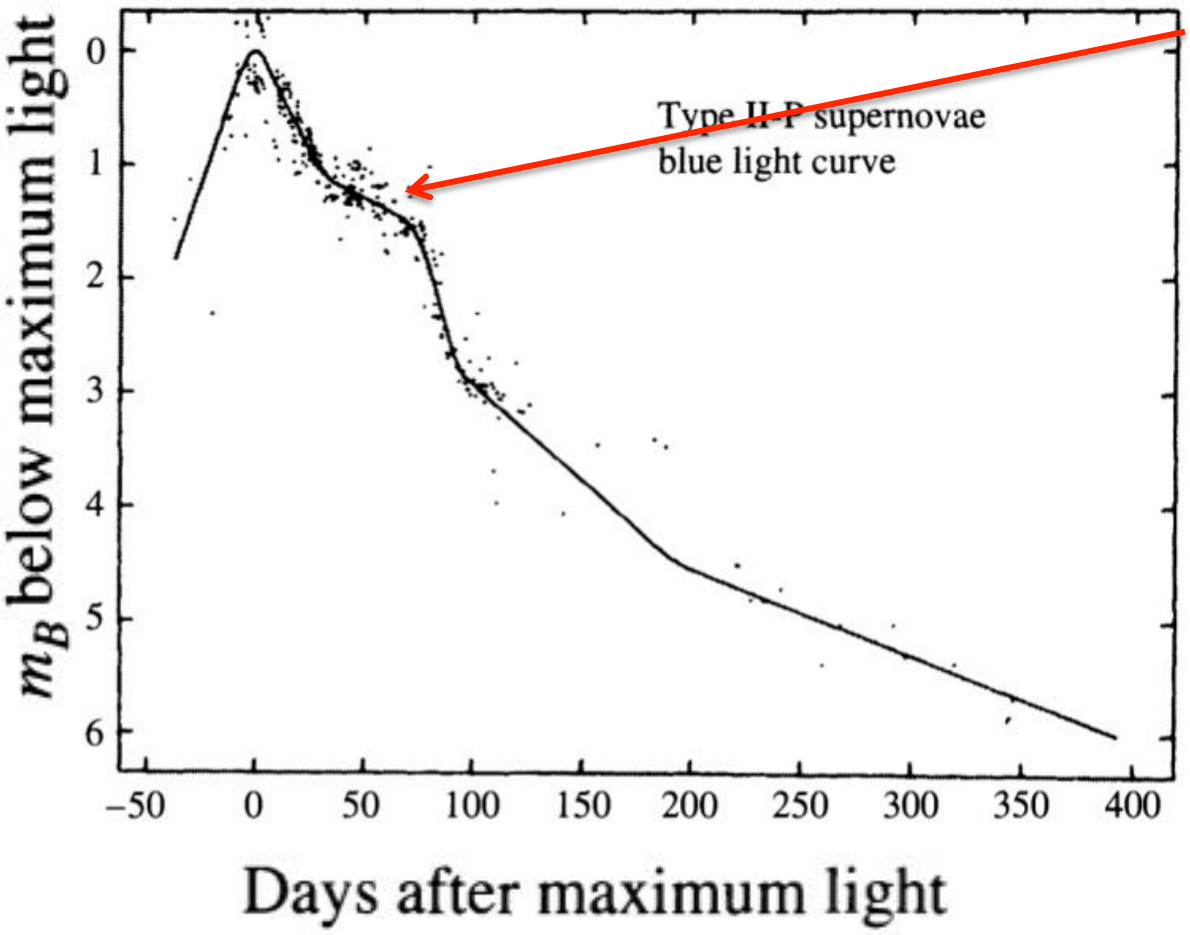

O *Plateau* é devido à energia depositada pelo frente de choque no envelope rico em hidrogênio → ionização → recombinação, liberando energia a uma T ~ 5000 K

Também energia do decaimento radioativo do Ni-56 ($\tau_{½}$ = 6,1 dias)

Na expansão do frente de choque da SN, diferentes isótopos podem ser formados. Vários deles são radioativos. Além do Ni-56 ($\tau_{1/2}$ = 6,1 dias), temos o decaimento de outros isótopos como Co-57 ($\tau_{1/2}$ = 271 dias), Na-22 ($\tau_{1/2}$ = 2,6 anos), Ti-44 ($\tau_{1/2}$ = 47 anos)

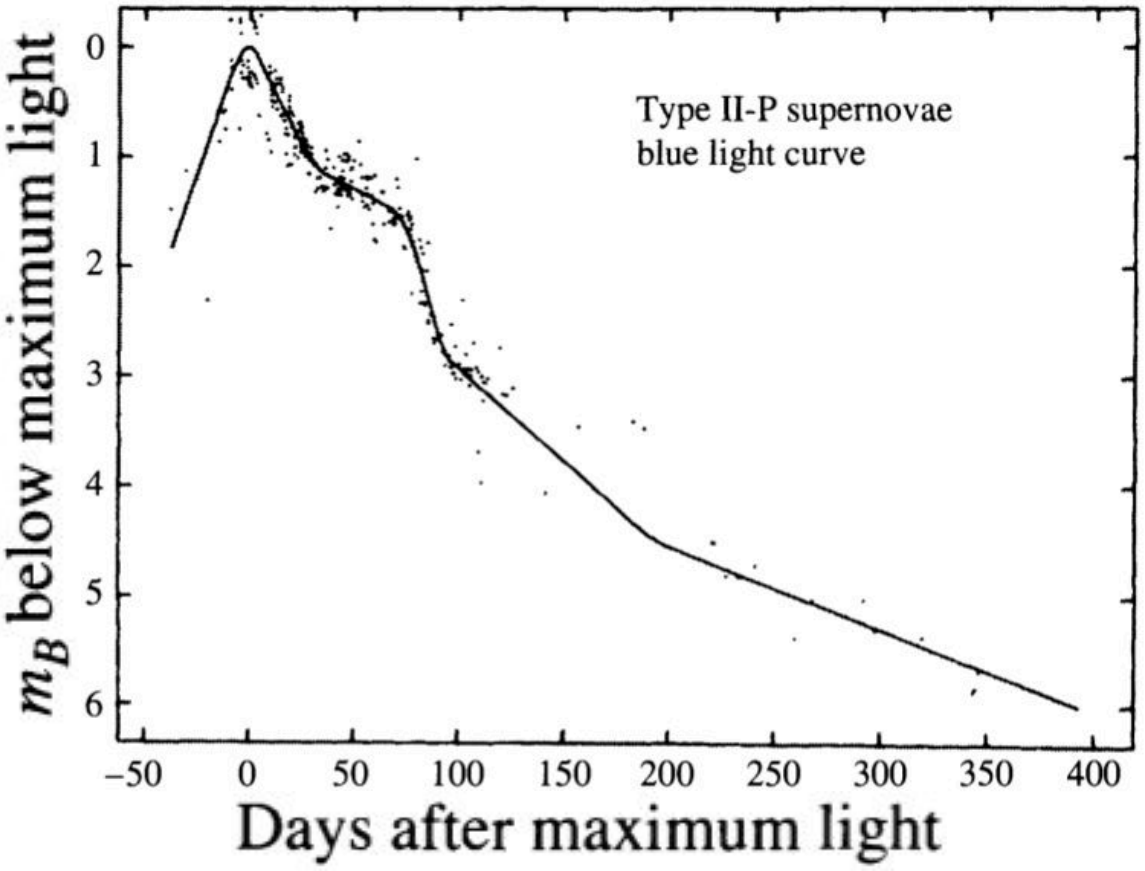

Isótopos abundantes dão forma à curva de luz da SN

$$^{56}_{28}\mathrm{Ni} \rightarrow {}^{56}_{27}\mathrm{Co} + e^{+} + \nu_e + \gamma$$ $\tau_{1/2}$ = 6,1 dias

$$^{56}_{27}\mathrm{Co} \rightarrow {}^{56}_{26}\mathrm{Fe} + e^{+} + \nu_e + \gamma$$ $\tau_{1/2}$ = 271 dias

Taxa de Decaimento radioativo:

$$\frac{dN}{dt} = -\lambda N$$

N: número de átomos
λ: constante de desintegração

$$N(t) = N_0 e^{-\lambda t}$$

$$\lambda = \frac{\ln 2}{\tau_{1/2}}$$

N_0: número inicial de átomos na amostra
$\tau_{1/2}$: tempo de vida média

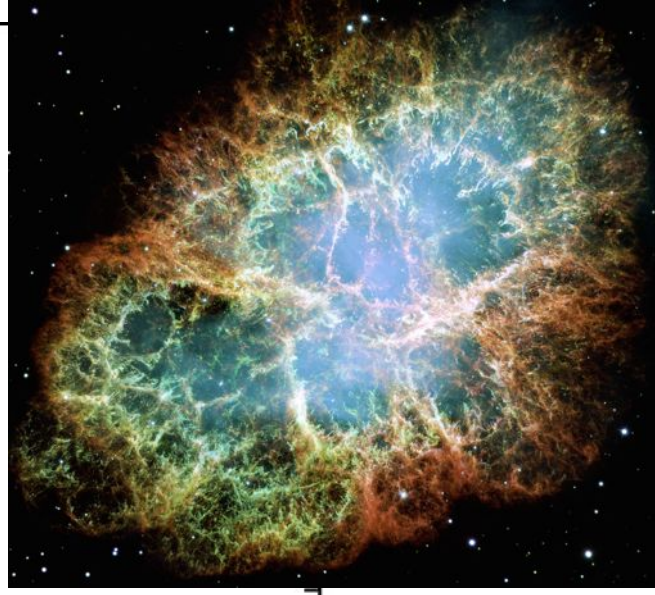

$$N(t) = N_0 e^{-\lambda t}$$

$$\lambda = \frac{\ln 2}{\tau_{1/2}}$$

$$^{56}_{28}\mathrm{Ni} \rightarrow {}^{56}_{27}\mathrm{Co} + e^{+} + \nu_e + \gamma$$

$\tau_{½}$ = 6,1 dias

50% chance de decaimento em 6,1 dias

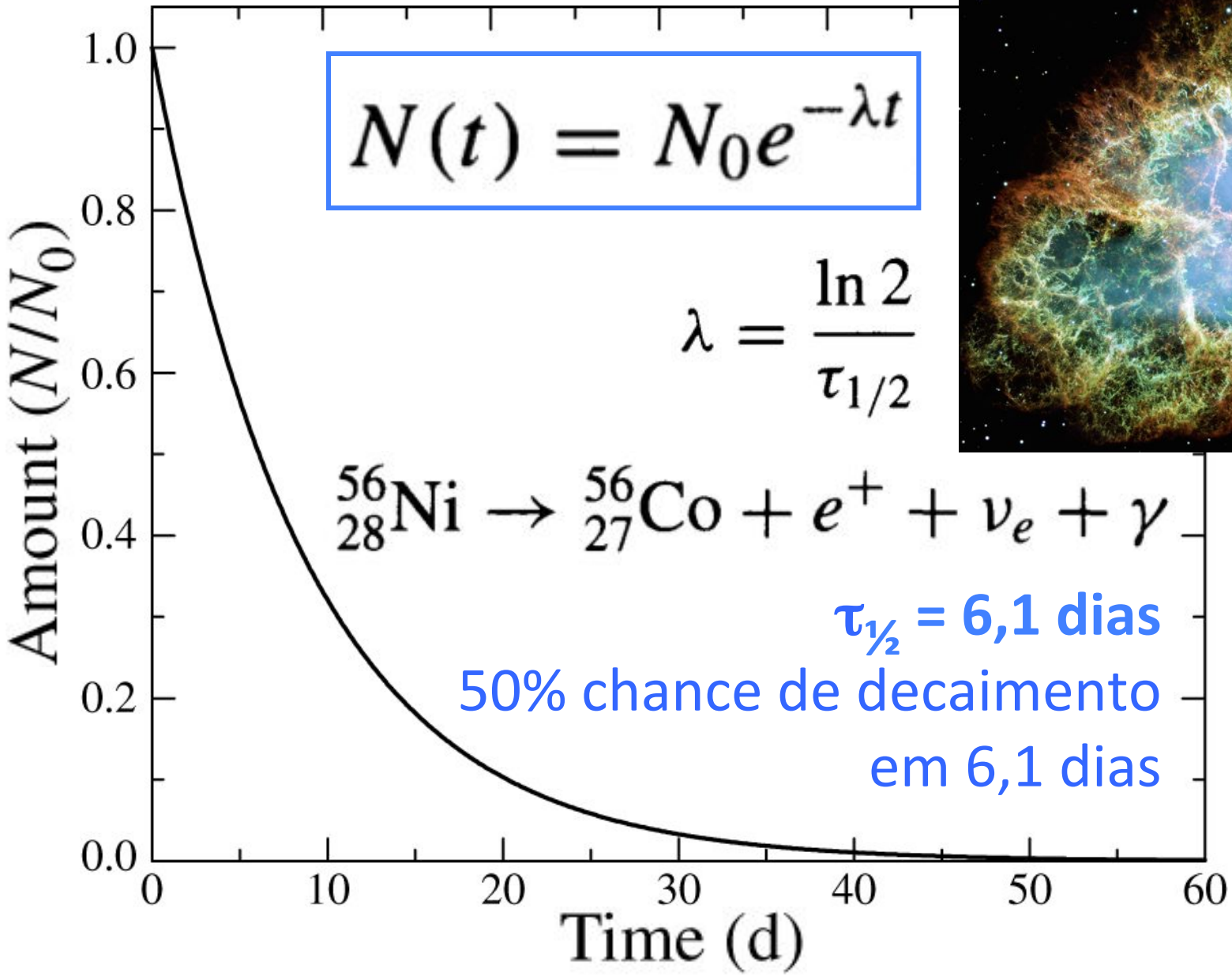

FIGURE 15.11 The radioactive decay of $^{56}_{28}$Ni, with a half-life of $\tau_{1/2} = 6.1$ days. There is a 50% chance that any given $^{56}_{28}$Ni atom will decay during a time interval of 6.1 days. If the original sample is entirely composed of $^{56}_{28}$Ni, after n successive half-lives the fraction of Ni atoms remaining is 2^{-n}.

A luminosidade deve ser proporcional a dN/dt

A taxa de variação da luminosidade (curva de luz): $$\frac{d \log_{10} L}{dt} = -0.434\lambda$$

Relação acima pode ser obtida usando:

$$\frac{dN}{dt} = -\lambda N$$

$$\frac{d \log_{10} L}{dt} = -\log_{10} e \cdot \lambda = -0.434\lambda$$

$u = f(x)$ is a function of x,

$$y = \log_b u$$

$$\frac{dy}{dx} = (\log_b e)\frac{u'}{u}$$

Ou: $$\frac{dM_{\text{bol}}}{dt} = 1.086\lambda$$

Medindo a inclinação da curva de luz podemos determinar λ

→ determinar a origem

$$\lambda = \frac{\ln 2}{\tau_{1/2}}$$

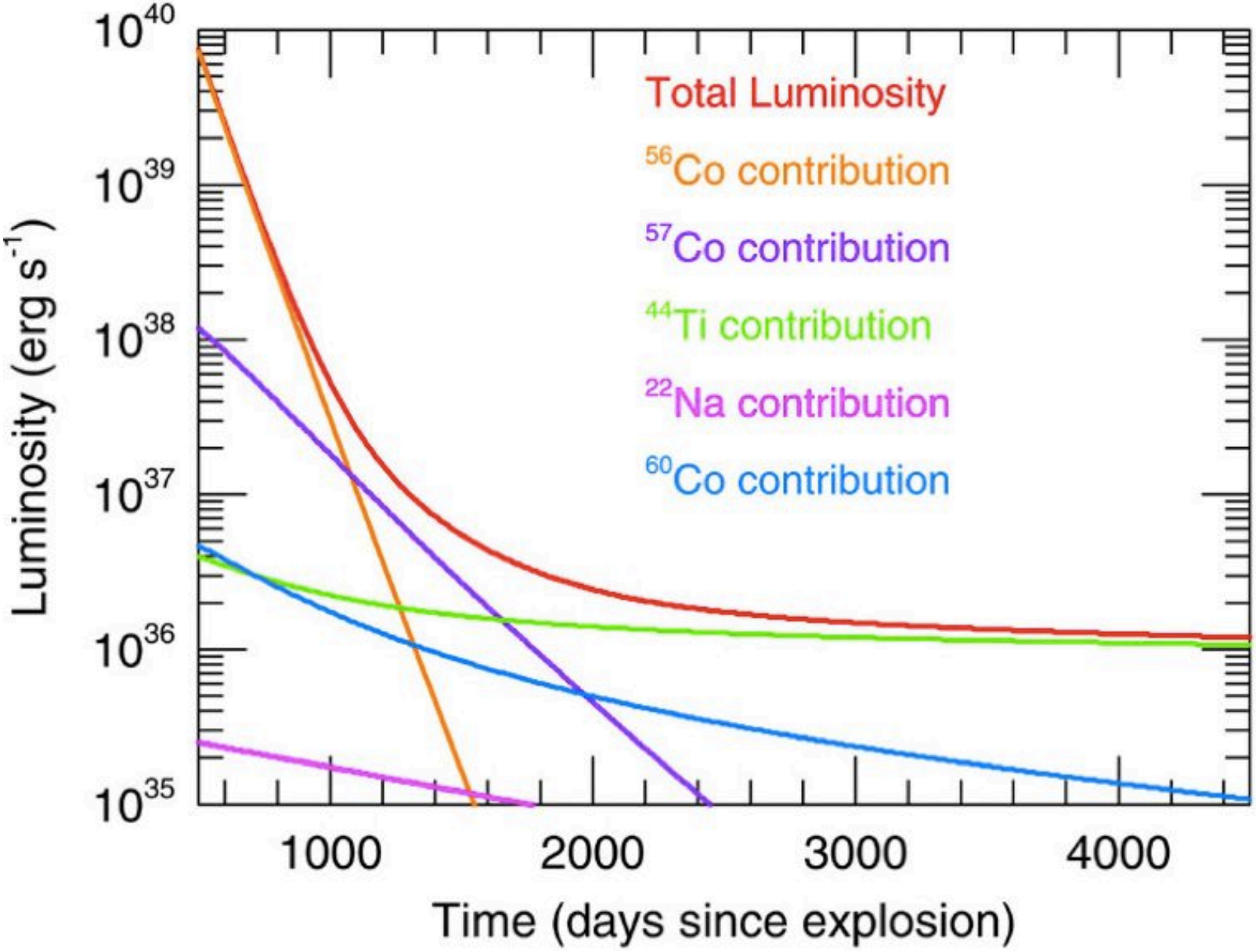

Radioactive decays contributing to supernova light curves. (From http://cococubed.asu.edu, Frank Timmes's pages at Arizona State University).

M_{bol} (pico) = -15,5, mas geralmente as tipo II têm -18

Demorou muito em chegar ao máximo

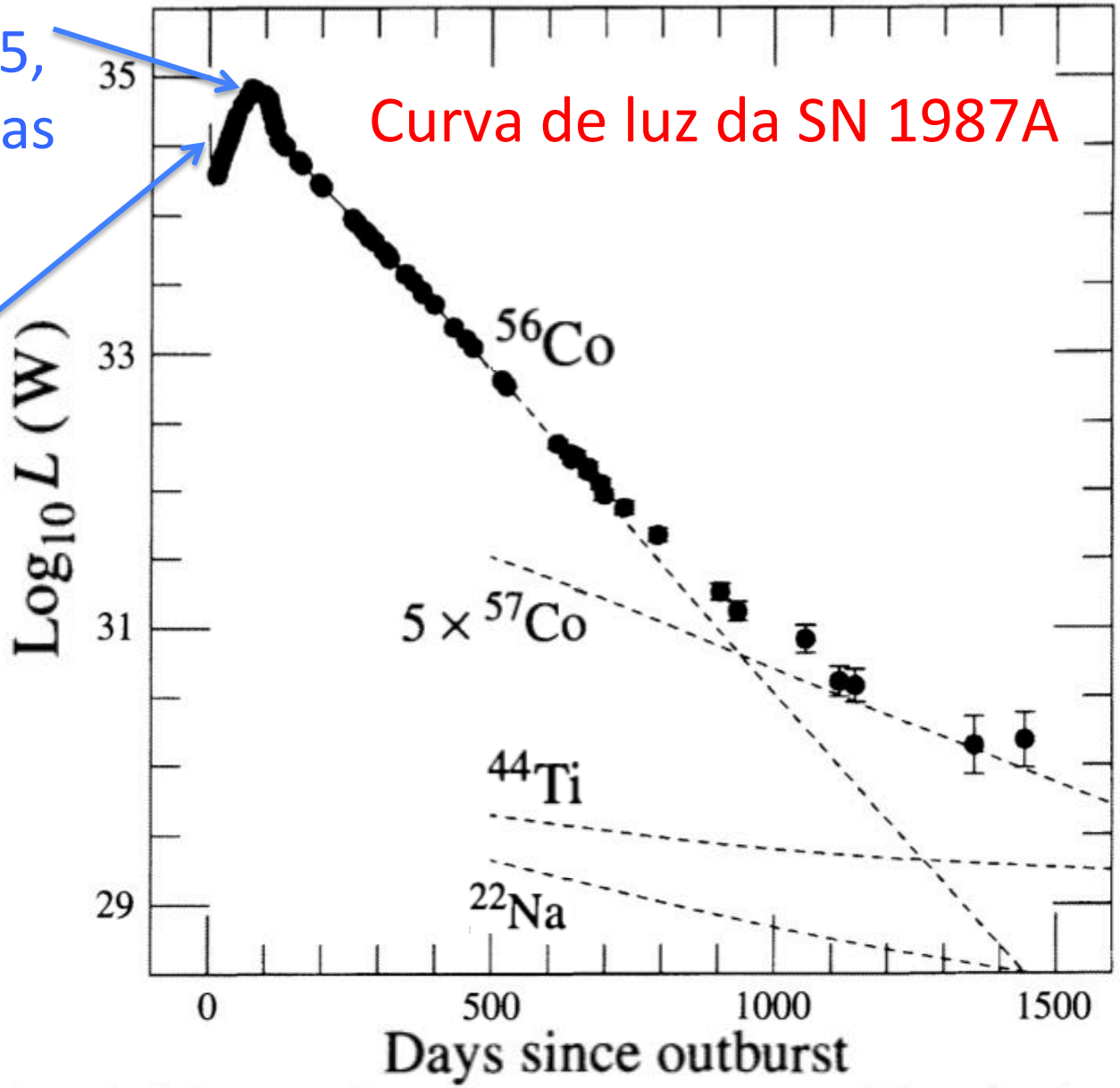

FIGURE 15.12 The bolometric light curve of SN 1987A through the first 1444 days after the explosion. The dashed lines show the contributions expected from the radioactive isotopes produced by the shock wave. The initial masses are estimated to be $^{56}_{28}$Ni (and later $^{56}_{27}$Co), 0.075 $M_\odot$; $^{57}_{27}$Co, 0.009 $M_\odot$ (five times the solar abundance); $^{44}_{22}$Ti, 1×10^{-4} $M_\odot$; and $^{22}_{11}$Na, 2×10^{-6} $M_\odot$. (Figure

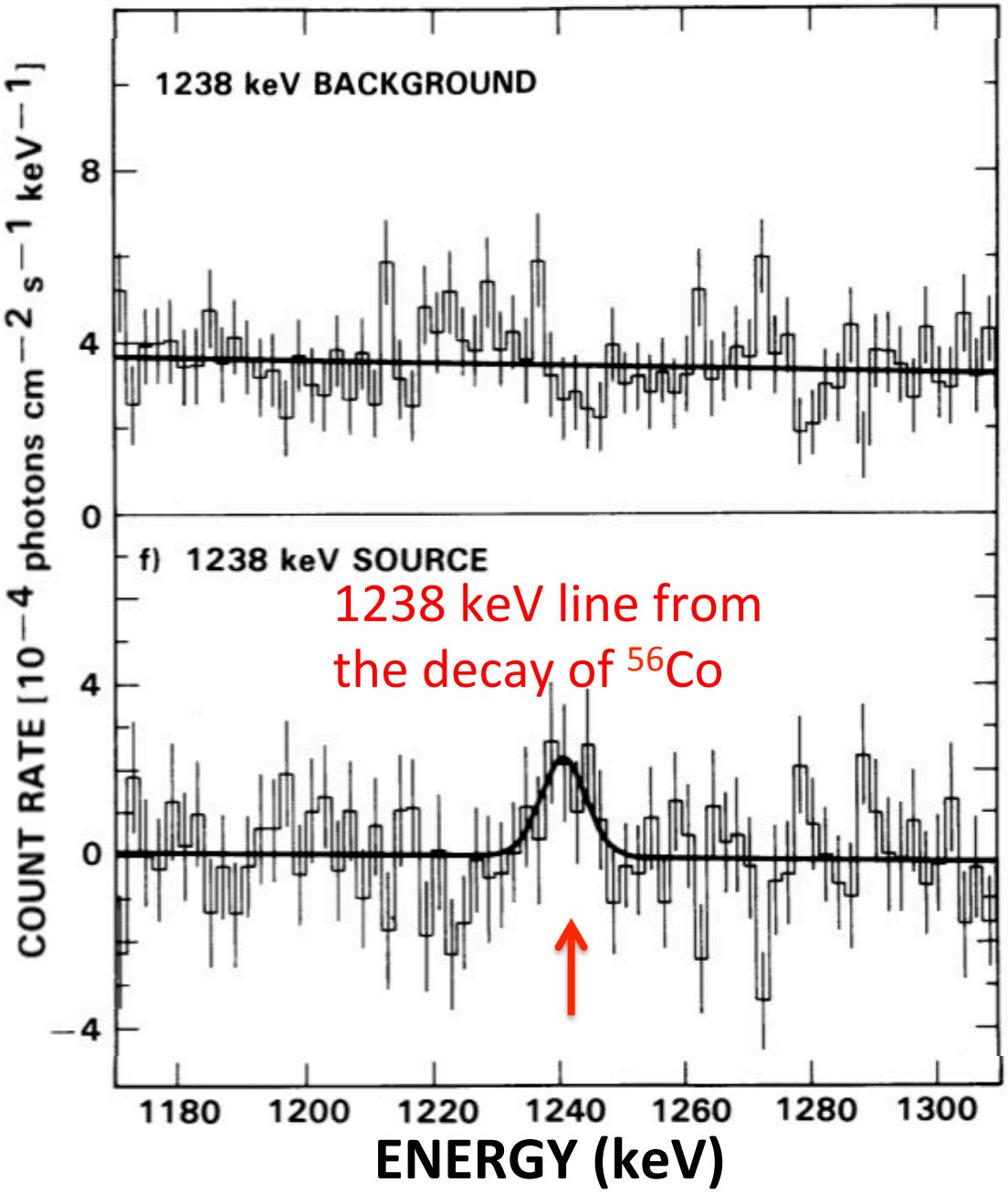

Gamma-ray observations of ^{56}Co in SN 1987A

Mahoney et al. 1988, ApJ, 334, L81

Supernova 1987A,

V ~ 2,9; d ~ 51,4 kpc

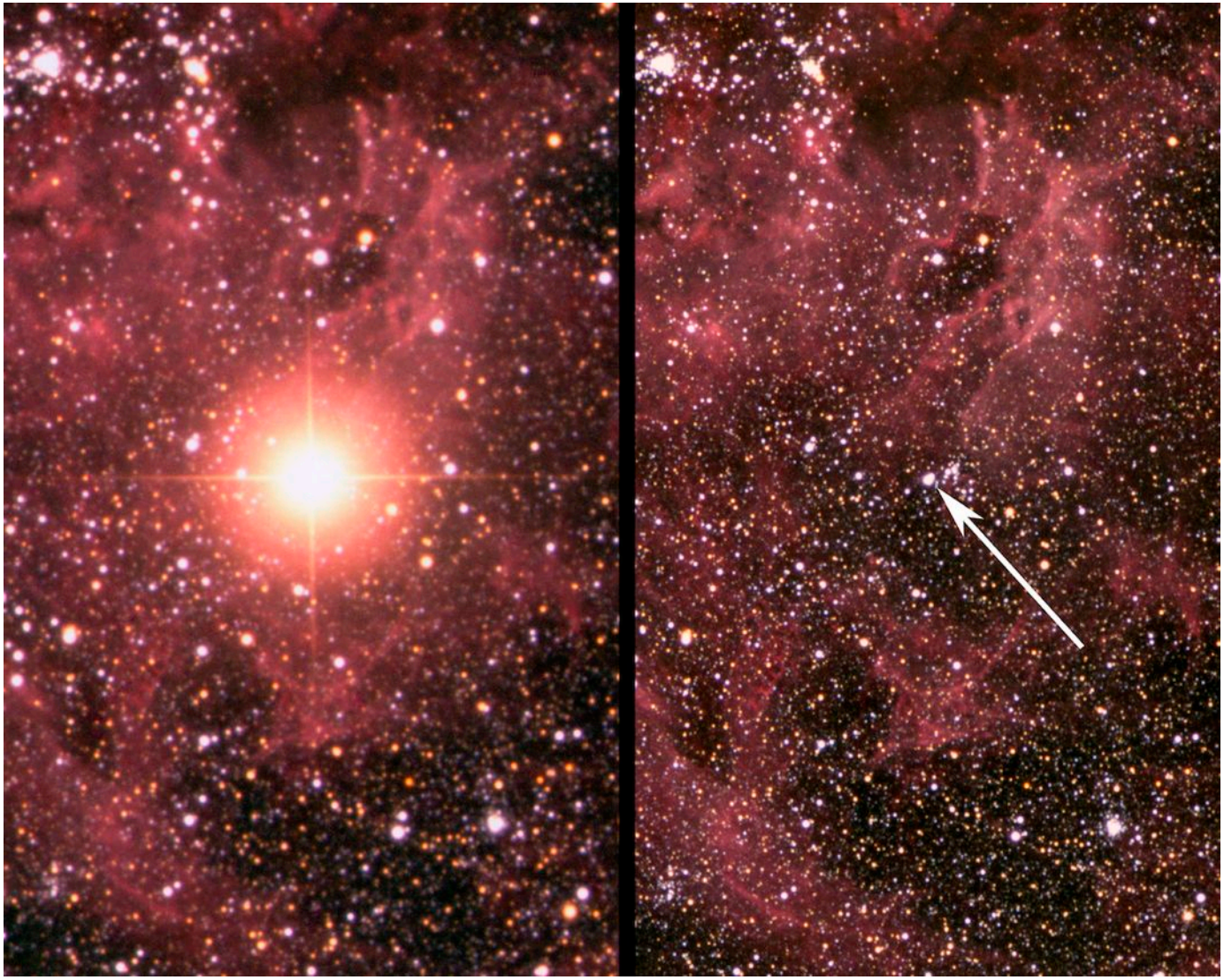

The progenitor star was identified as Sanduleak −69° 202, a blue supergiant, B3I (V = 12)

T = 16 000 K

$L = 1{,}1 \times 10^5 L_{Sol}$

Supernova 1987A after exploding & an image before the explosion. (c) David Malin / AAO

Estrela progenitora da Supernova 1987A

Supernova 1987A

Massa inicial ~ 20 M_{Sol}

Remanescente de supernova

Supernova 1054

Still expanding at rate of 1450 km/s

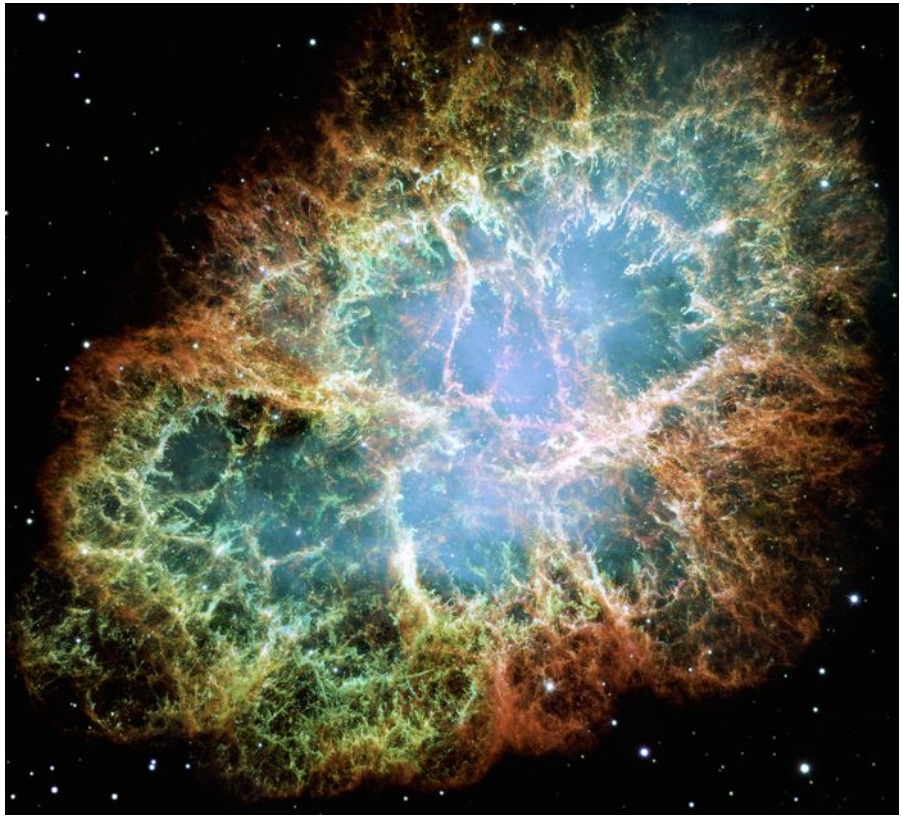

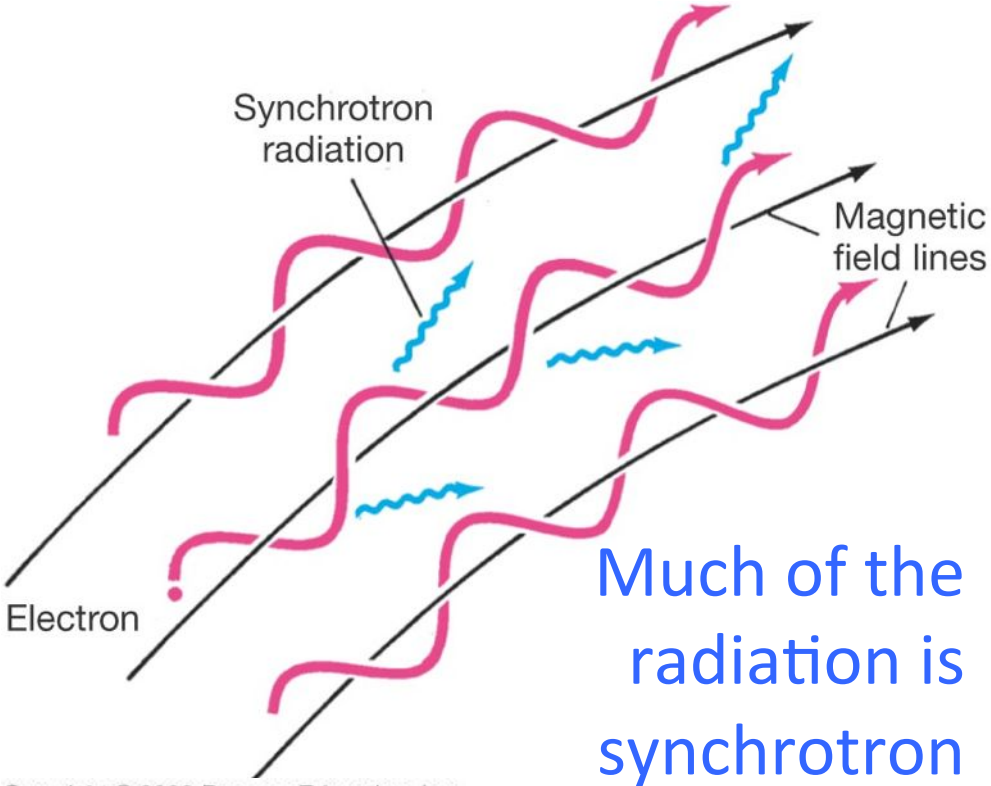

Copyright © 2008 Pearson Education, Inc.,

Much of the radiation is synchrotron

There are now many examples of **supernova remnants** (SNR), including the Crab Nebula, located in the constellation of Taurus (recall Fig. 15.4). Today, nearly 1000 years since the SN 1054 explosion, the Crab is still expanding at a rate of almost 1450 km s^{-1} and it has a luminosity of 8×10^4 $L_\odot$. Much of the radiation being emitted is in the form of highly polarized synchrotron radiation (see Section 4.3), indicating the presence of relativistic electrons that are spiraling around magnetic field lines.

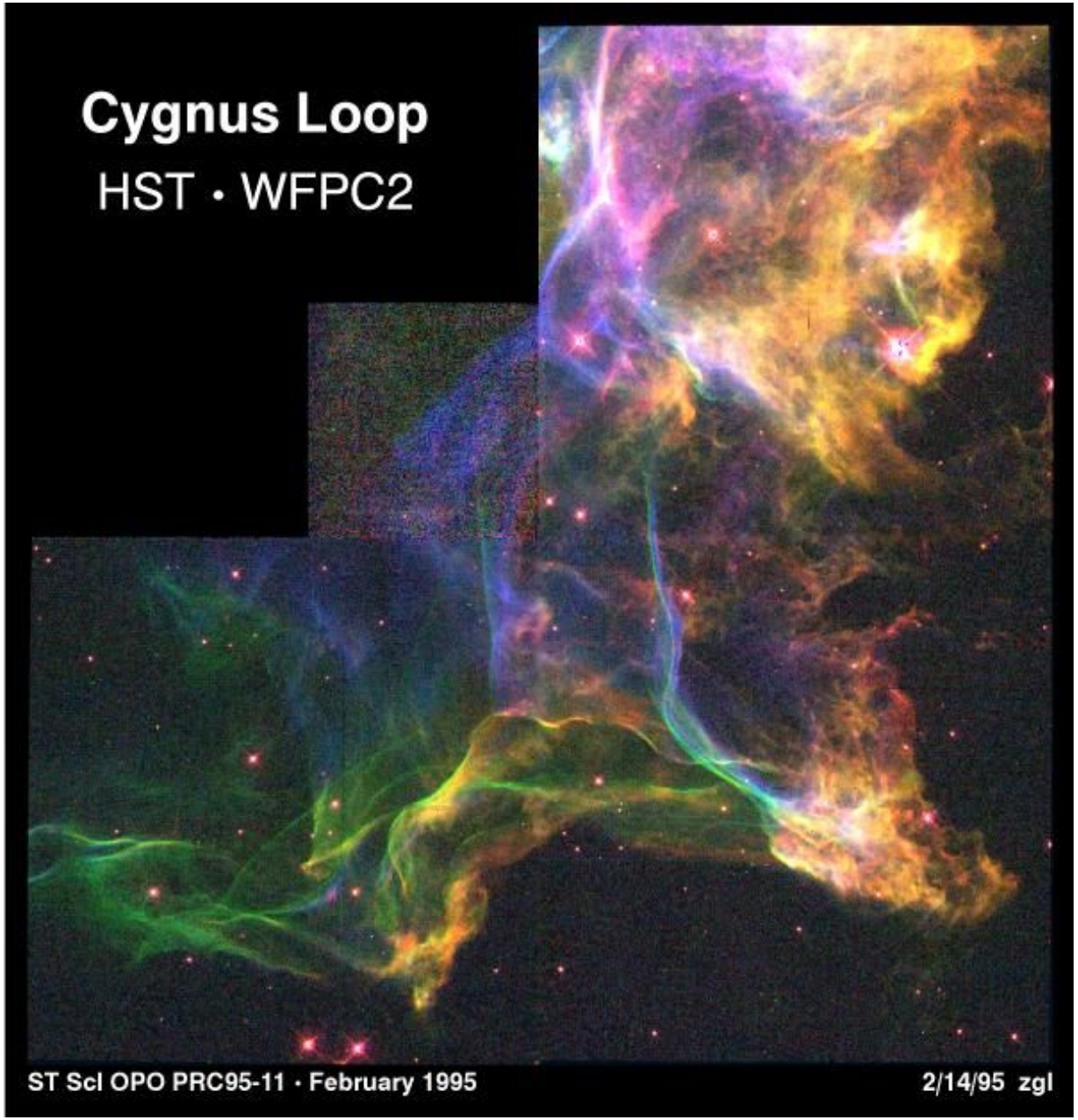

Pequena parte do Cygnus loop, nebulosa de 15 000 anos

Ionização do ISM quando o remanescente SN encontra o ISM

FIGURE 15.13 An HST WF/PC 2 image of a portion of the Cygnus Loop, 800 pc away.

The Mysterious Rings of Supernova 1987A, © HST

Both rings (inner ring and 2 outer rings) may be due to previous mass loss

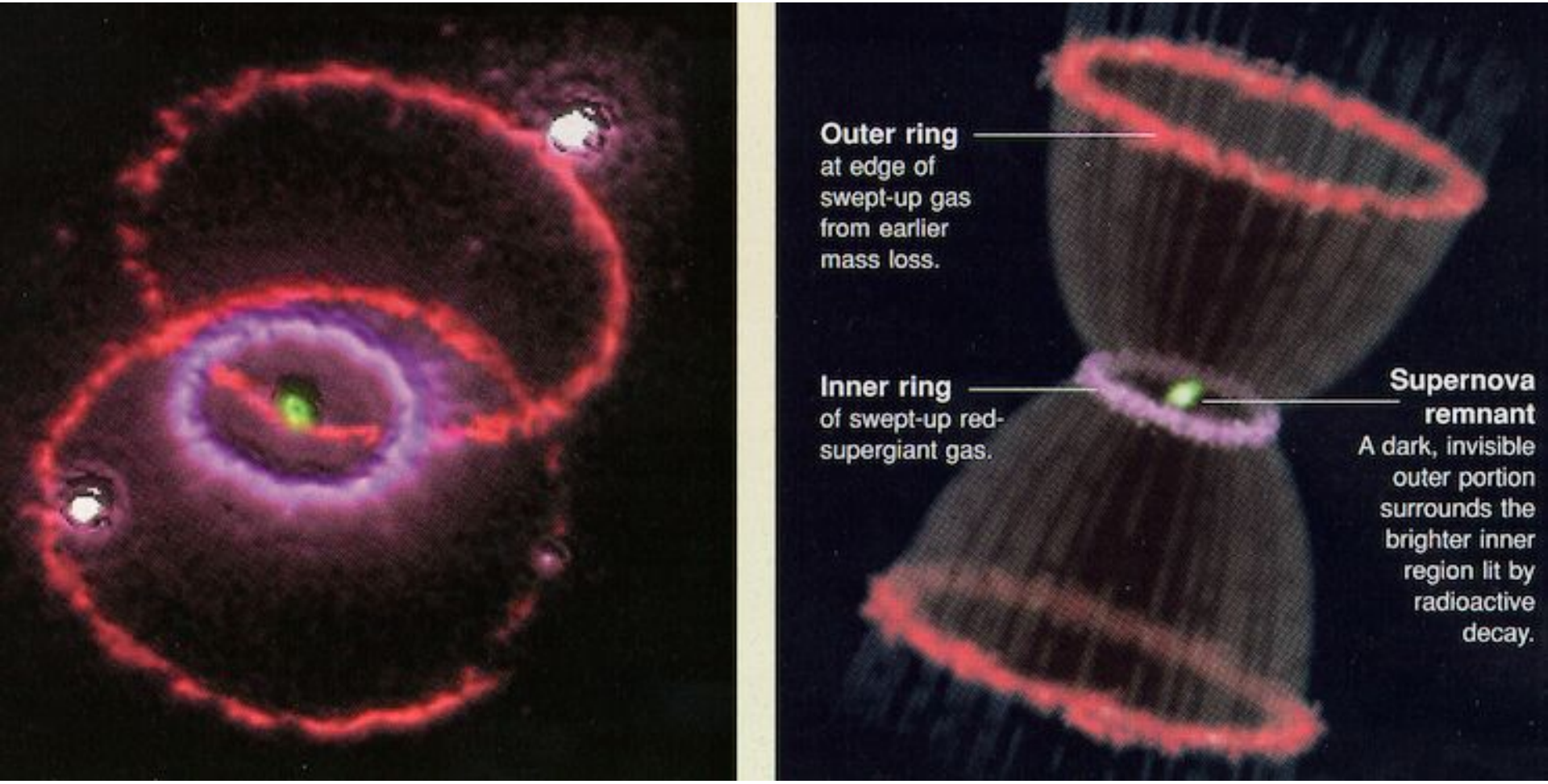

© Sky & Telescope

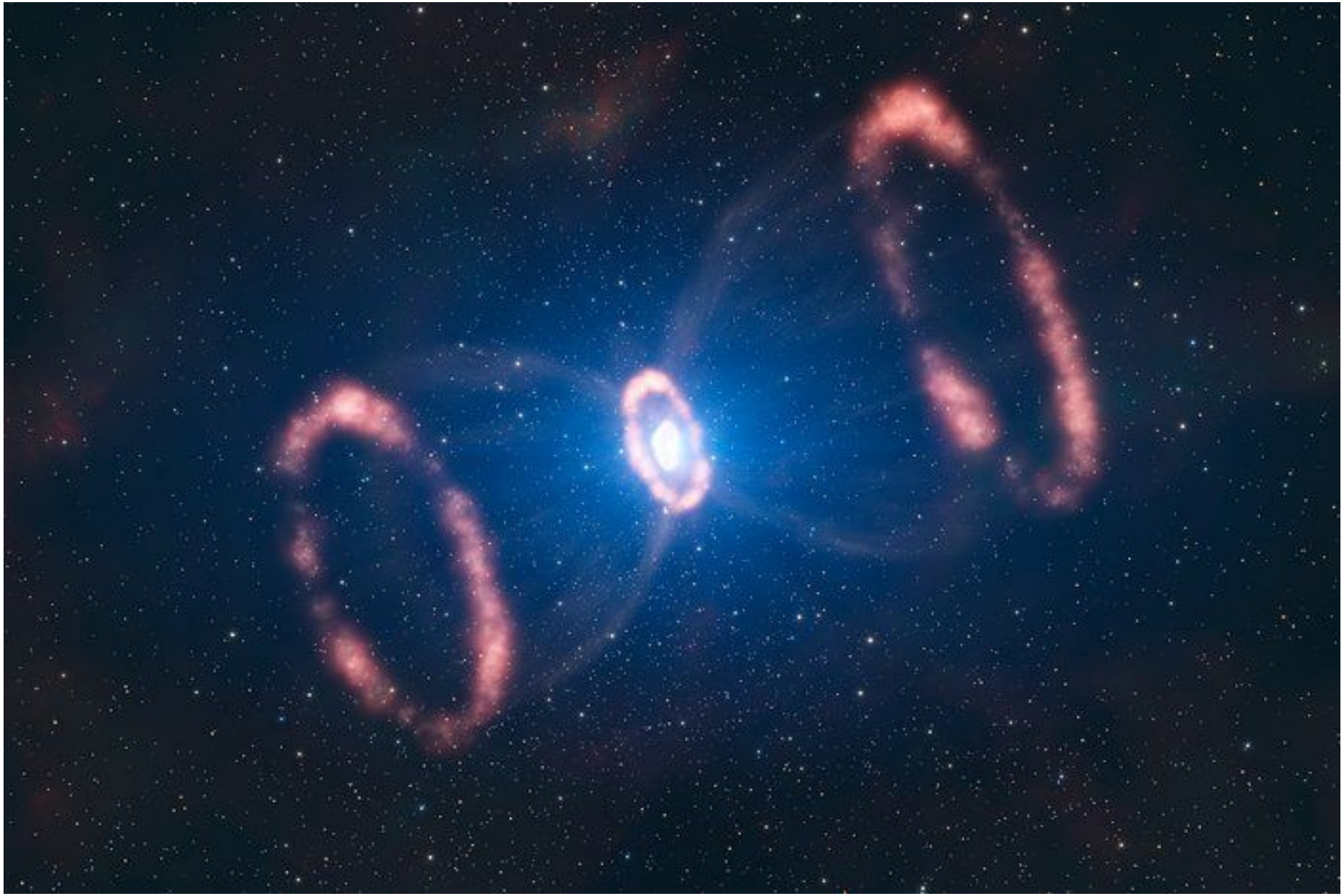

Artist’s impression of SN 1987A. © ESO

http://www.eso.org/public/brazil/news/eso1032/

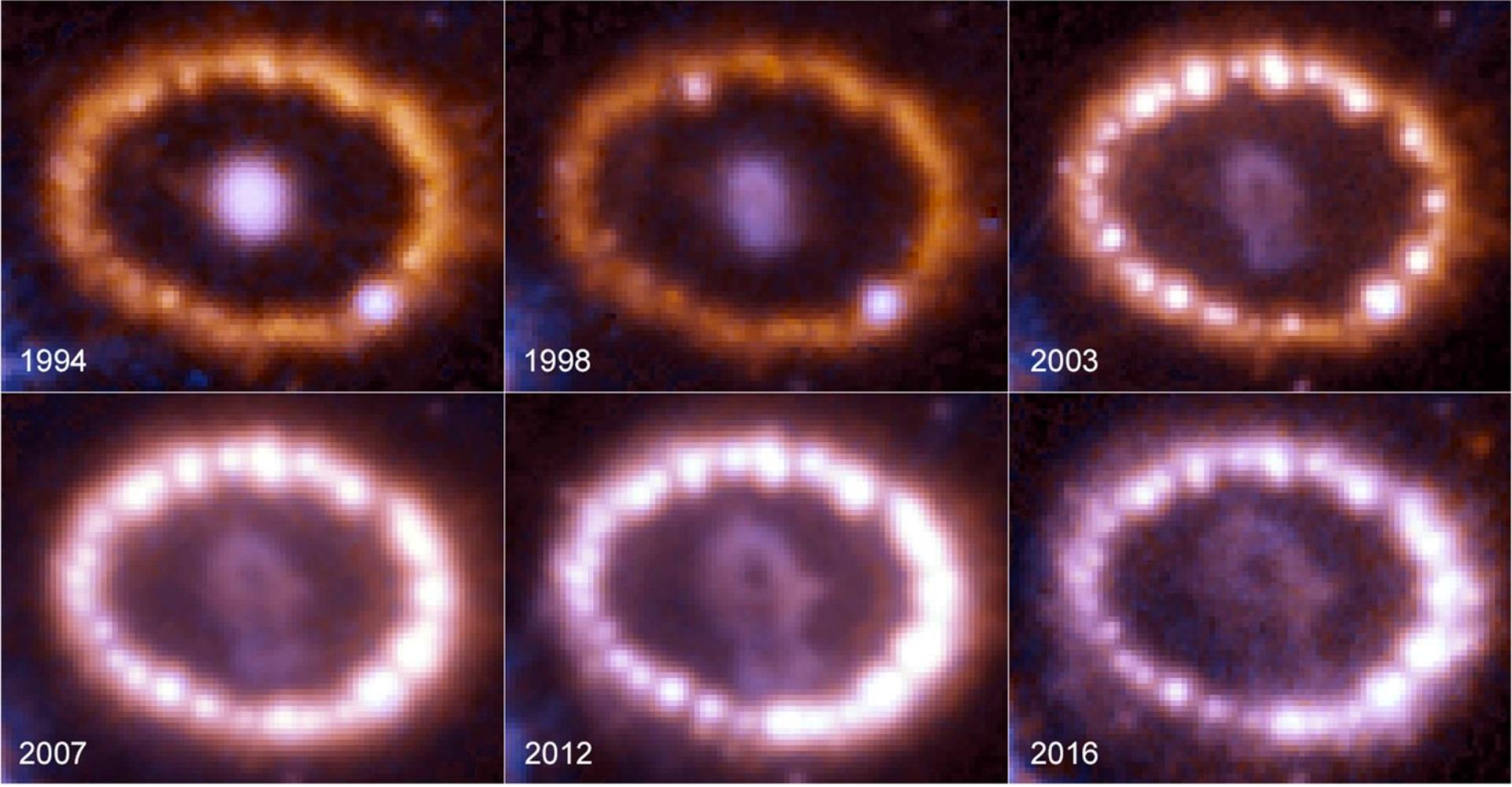

HST/NASA images (between 1994 and 2016) chronicle the brightening and fading of a ring of gas around an exploded star.

https://www.nasa.gov/feature/goddard/2017/the-dawn-of-a-new-era-for-supernova-1987a

Evolution of the ring collision from 1994 to 2014 (days 2270–9975) from a combination of *HST* B- and R-band images. Fransson et al. (2015)

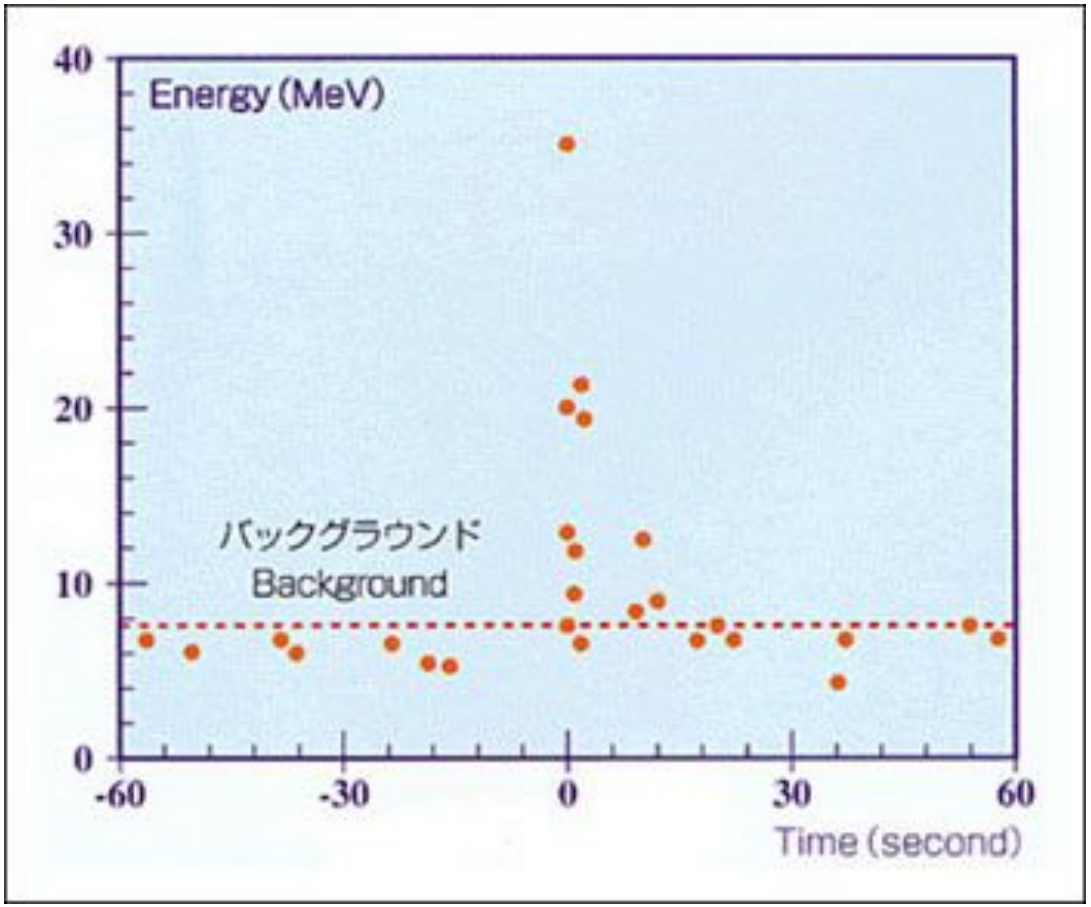

Kamiokande (large water Cherenkov detector) detected 11 events of neutrinos from the SN 1987A

http://www-sk.icrr.u-tokyo.ac.jp/sk/physics/supernova-e.html

8 events were also detected in the USA.

Both neutrino detections occurred hours before the optical detection → neutrinos must have travelled close to *c*.

The Search for a Compact Remnant of SN 1987A

Interestingly, as of 2006, neutrinos have been the only direct evidence of the formation of a compact object at the center of SN 1987A. All attempts to detect a remnant in optical, ultraviolet, or X-ray wavelengths have failed. In addition, efforts to find any evidence of a surviving binary companion have also been unsuccessful. The upper limit on the luminosity in the optical portion of the electromagnetic spectrum is currently less than 8×10^{26} W, equivalent to the optical energy output of an F6 main-sequence star. Ultaviolet spectra lead to an upper limit of $L_{UV} \leq 1.7 \times 10^{27}$ W, and Chandra has set an upper limit on the X-ray luminosity of $L_X \leq 5.5 \times 10^{26}$ W in the energy band between 2 and 10 keV.

2017: objeto compacto ainda não encontrado

The Remnant of Supernova 1987A

Annual Review of Astronomy and Astrophysics

Vol. 54:19-52 (Volume publication date September 2016)
First published online as a Review in Advance on June 27, 2016
https://doi.org/10.1146/annurev-astro-082615-105405

Richard McCray[1] and Claes Fransson[2]

[1]Department of Astronomy, University of California, Berkeley, California 94720-3411; email: mccrayr@me.com
[2]Department of Astronomy, The Oskar Klein Centre, Stockholm University, Stockholm 10691, Sweden; email: claes@astro.su.se

Abundâncias químicas no universo

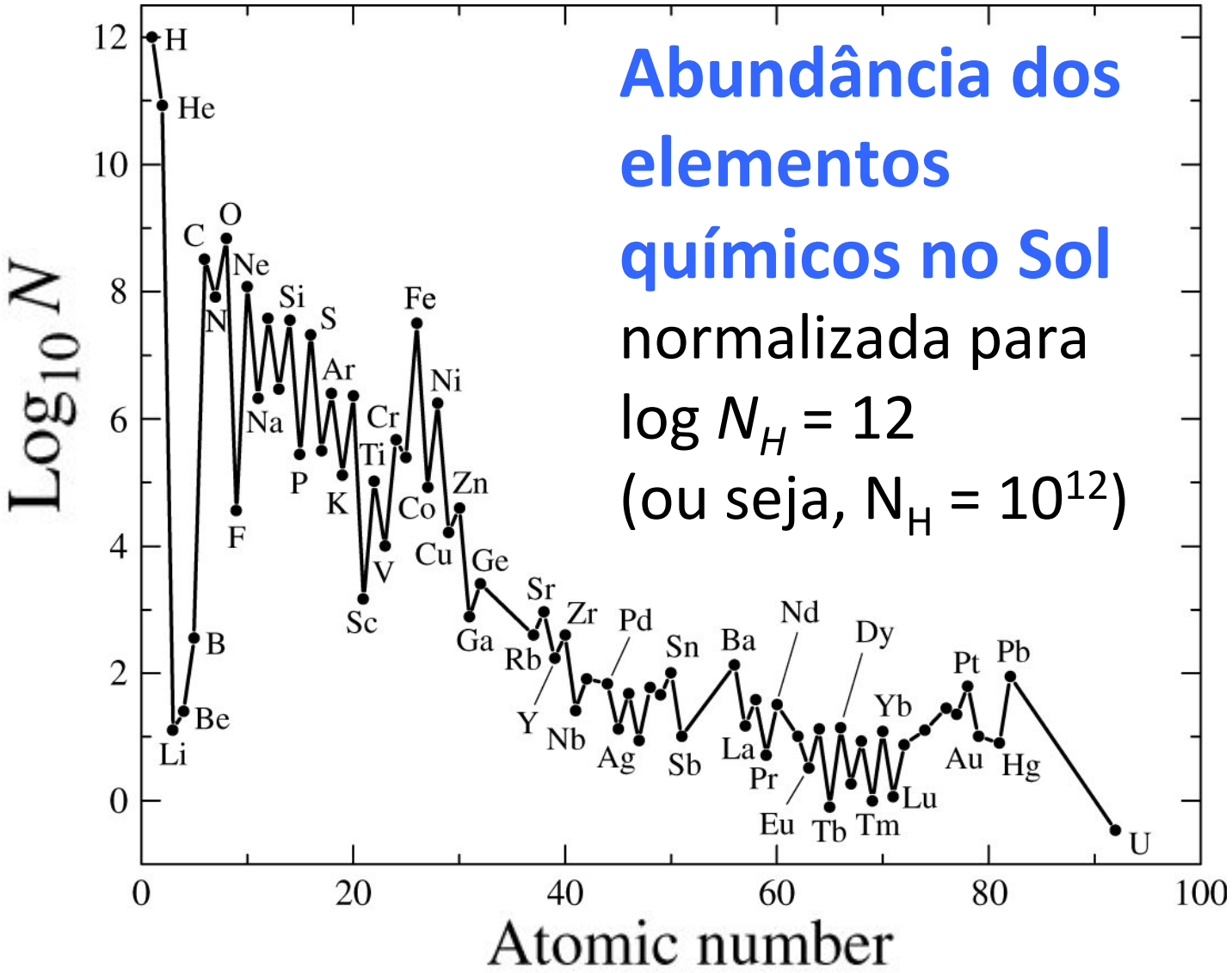

H, He: muito abundantes.

Li, Be, B: pouco abundantes

FIGURE 15.16 The relative abundances of elements in the Sun's photosphere. All abundances are normalized relative to 10^{12} hydrogen atoms. (Data from Grevesse and Sauval, *Space Sci. Rev.*, *85*, 161, 1998.)

Evolução de nosso universo
Primeiros minutos: H, He (e pouco Li)

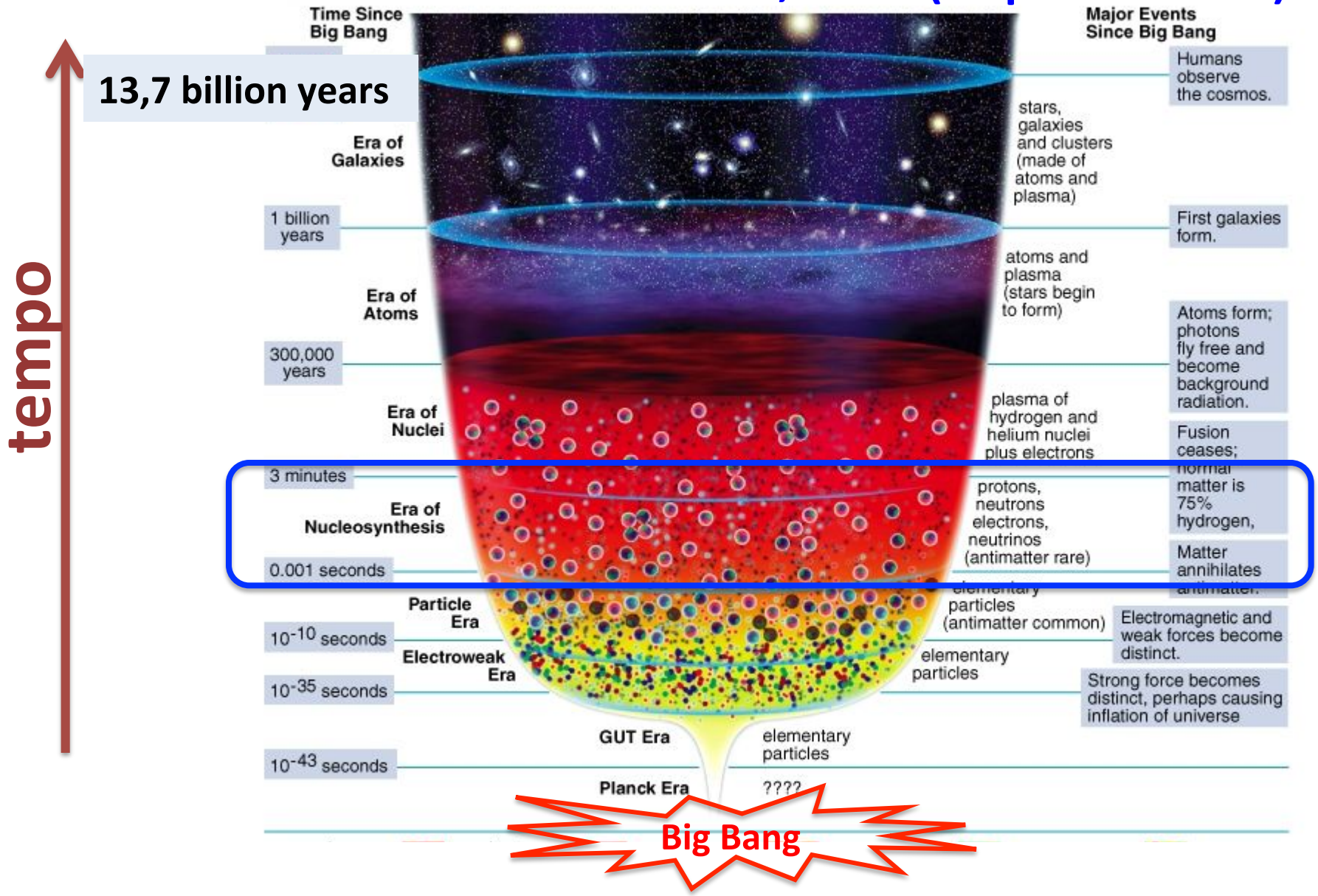

Nucleossíntese primordial

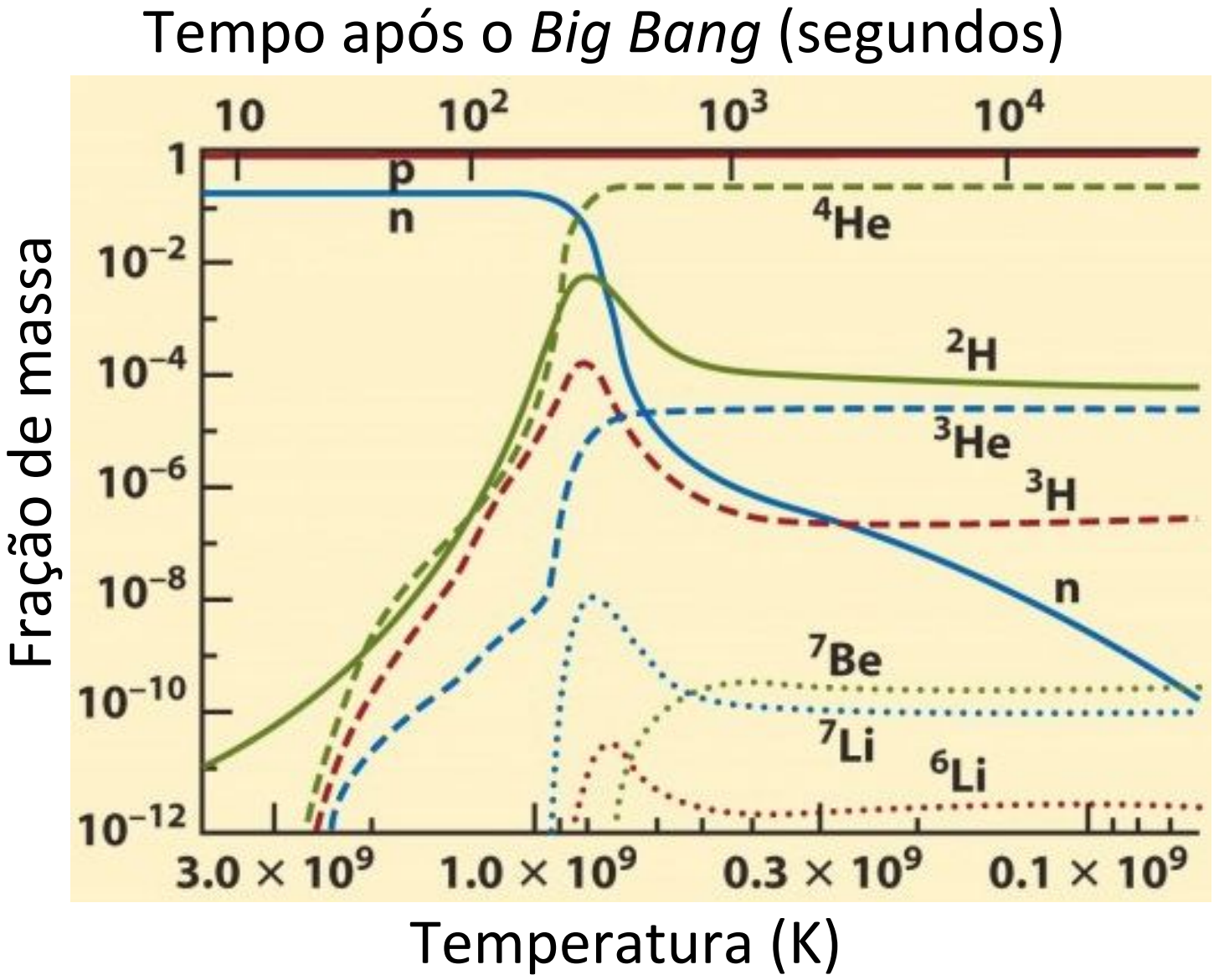

^{3}H e ^{7}Be não sobrevivem

^{3}H (trítio) decai → ^{3}He ($\tau_{½}$ = 2,6 anos)

^{7}Be decai → ^{7}Li ($\tau_{½}$ = 53 d)

https://universe-review.ca/F02-cosmicbg01.htm

Li e Be são facilmente destruídos em interiores estelares.

Li queima a $2{,}7 \times 10^6$ K e Be a $3{,}6 \times 10^6$ K

$$p + {}^{6}_{3}Li \rightarrow {}^{7}_{4}Be$$

$${}^{7}_{4}Be + e^{-} \rightarrow {}^{7}_{3}Li + \nu$$

$$p + {}^{7}_{3}Li \rightarrow {}^{8}_{4}Be$$

$${}^{8}_{4}Be \rightarrow 2\,{}^{4}_{2}He + energia$$

De fato, a abundância de Li no Sol é 150 vezes menor do que em meteoritos, porem o Be no Sol é similar ao dos meteoritos.

→ processos de transporte no envelope convectivo atingem a região de queima de Li mas não atingem a região onde Be é queimado

Be & Li no Sol e em estrelas gêmeas do Sol

Marcelo Tucci Maia et al. 2015, A&A 576, L10

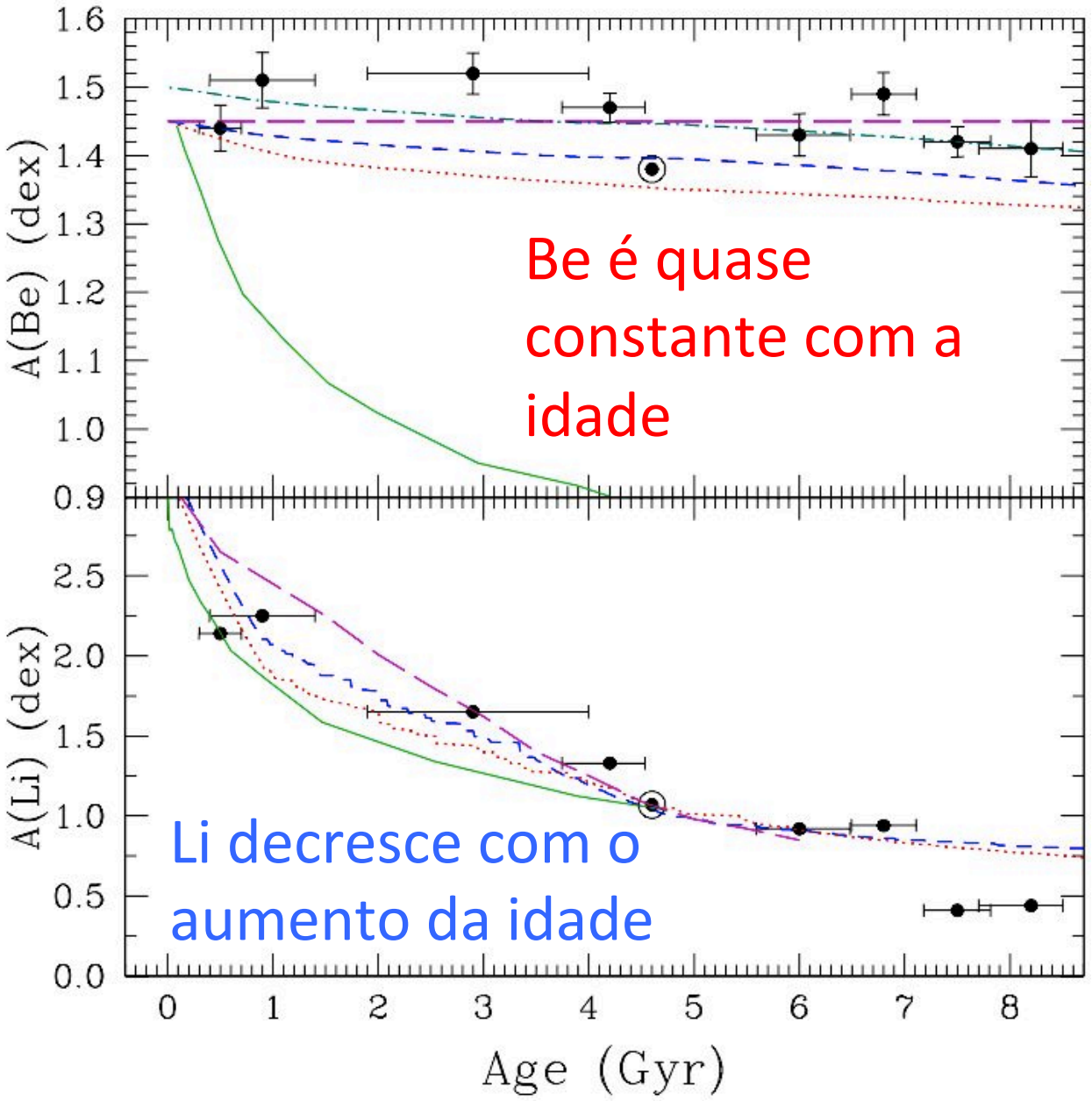

Os processos de transporte atingem apenas a camada de queima do Li, logo abaixo da zona convectiva (não chegam à camada de queima de Be que é mais interna)

Abundâncias químicas no Sol

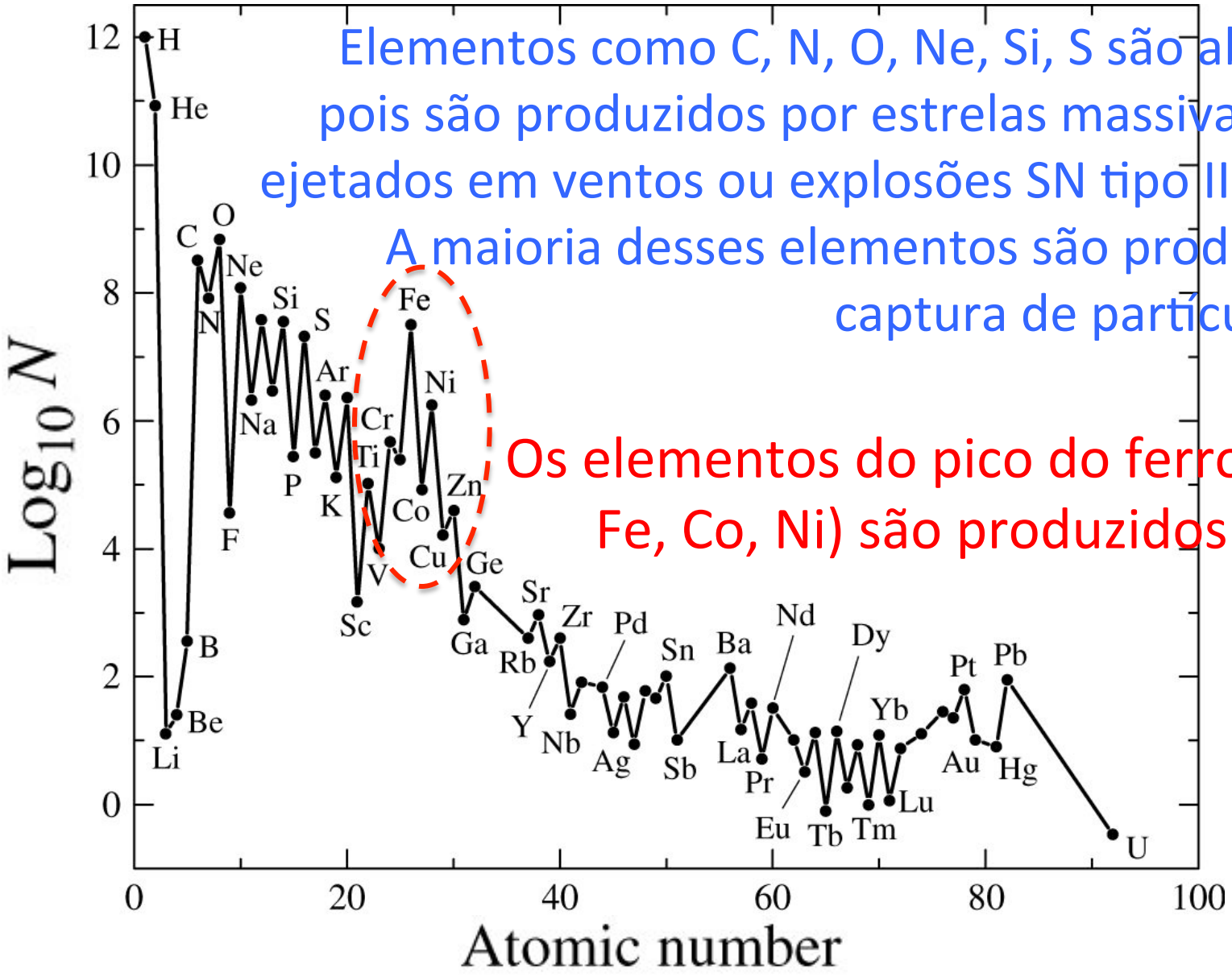

Elementos como C, N, O, Ne, Si, S são abundantes pois são produzidos por estrelas massivas e depois ejetados em ventos ou explosões SN tipo II (ou Ib/Ic).

A maioria desses elementos são produzidos por captura de partícula α (^{4}He)

Os elementos do pico do ferro (e.g., Cr, Fe, Co, Ni) são produzidos por SN Ia

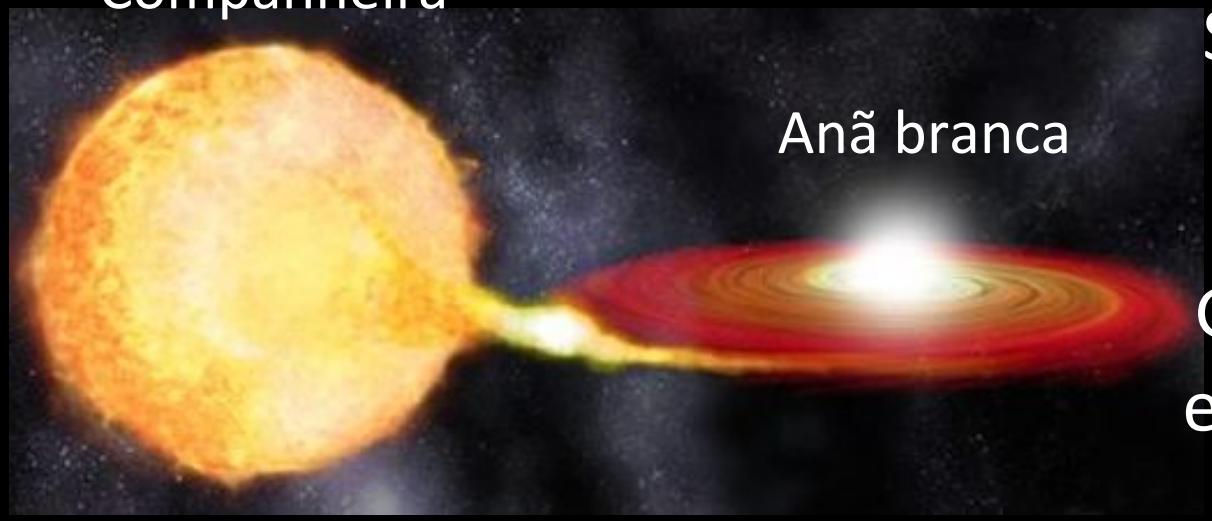

Supernovas de tipo Ia enriquecem quimicamente a Galáxia, em particular em elementos do pico do Fe.

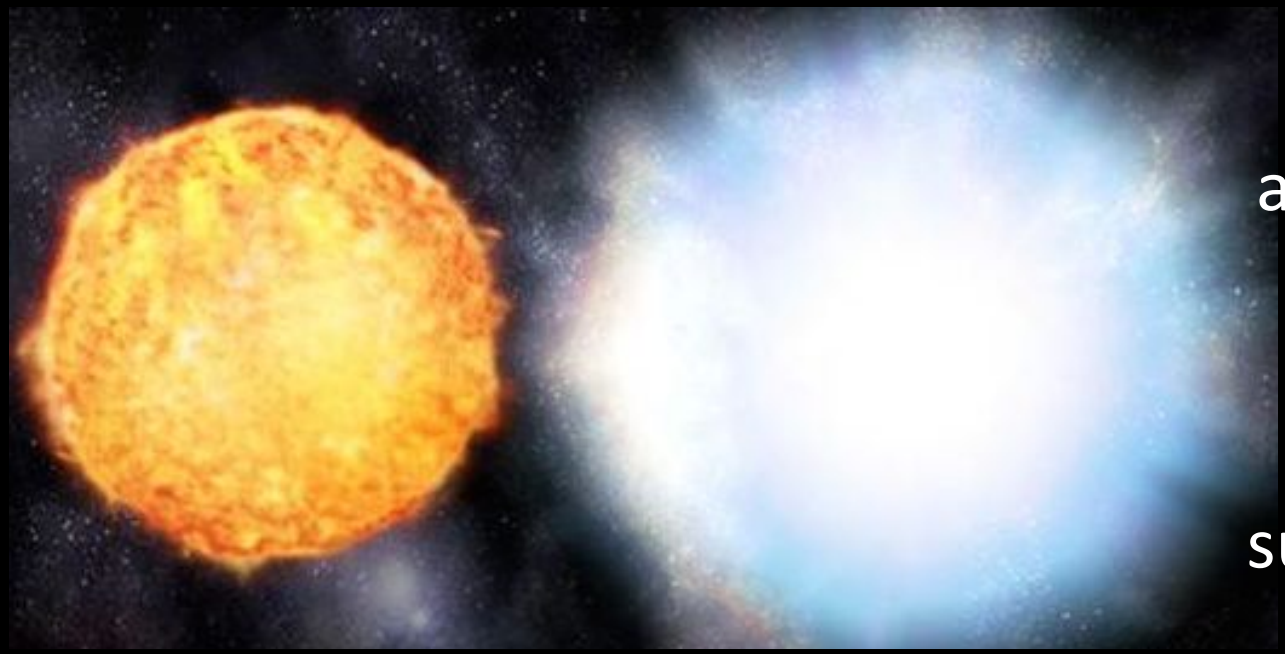

Acontecem quando anãs brancas (massa inicial < $8M_{Sol}$) acrescem massa de companheiras e superam certo limite (~1,4 M_{Sol})

https://phys.org/news/2014-08-ia-supernovae-stem-explosion-white.html

Para núcleos com alto Z fica mais difícil termos fusão nuclear devido à maior barreira Coulombiana

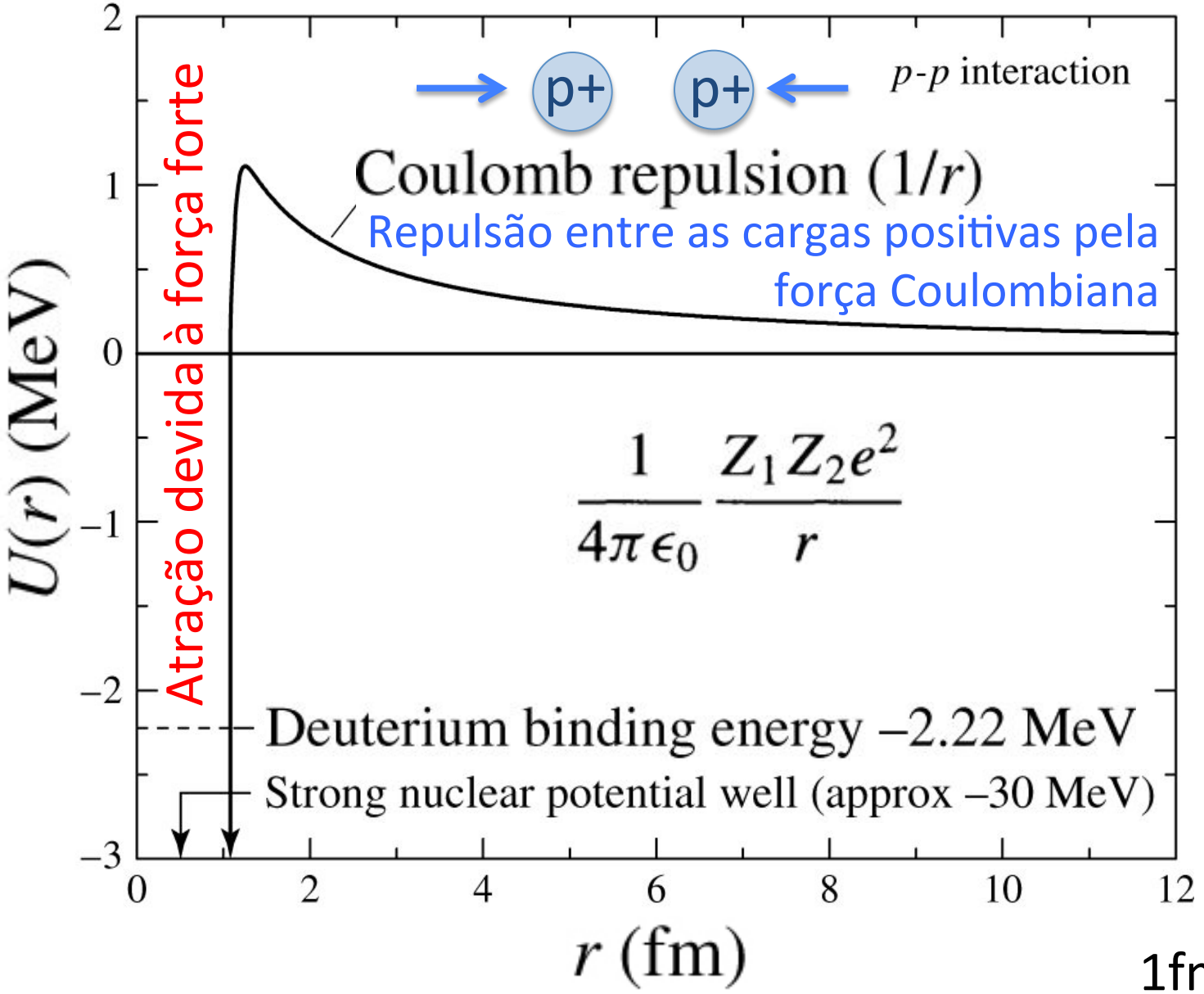

1fm = 10^{-15}m

Nucleossíntese por captura de nêutrons: processo-s e processo-r

Nêutrons não são afetados pela barreira Coulombiana.

$$^{A}_{Z}X + n \rightarrow {}^{A+1}_{Z}X + \gamma$$

O Nêutron capturado pode decair → elemento químico com Z = Z+1

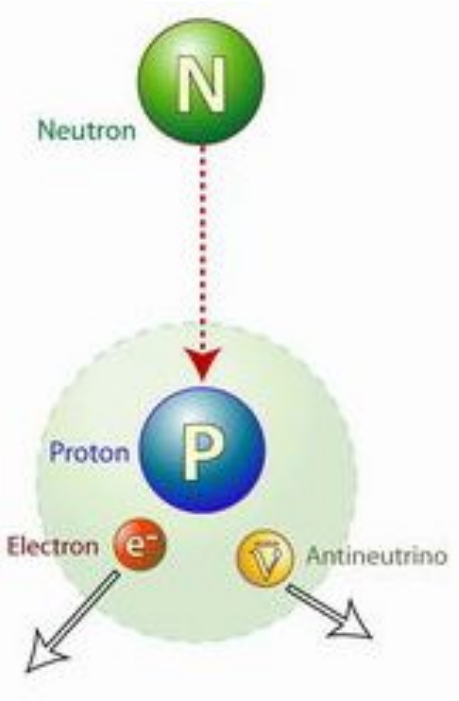

$$^{A+1}_{Z}X \rightarrow {}^{A+1}_{Z+1}X + e^{-} + \overline{\nu}_{e} + \gamma$$

Alto fluxo de nêutrons: processo-*r* (rapid)
E.g., SN II ou fusão de estrelas de nêutrons

Baixo fluxo de nêutrons: processo-*s* (slow)
Estrelas AGB

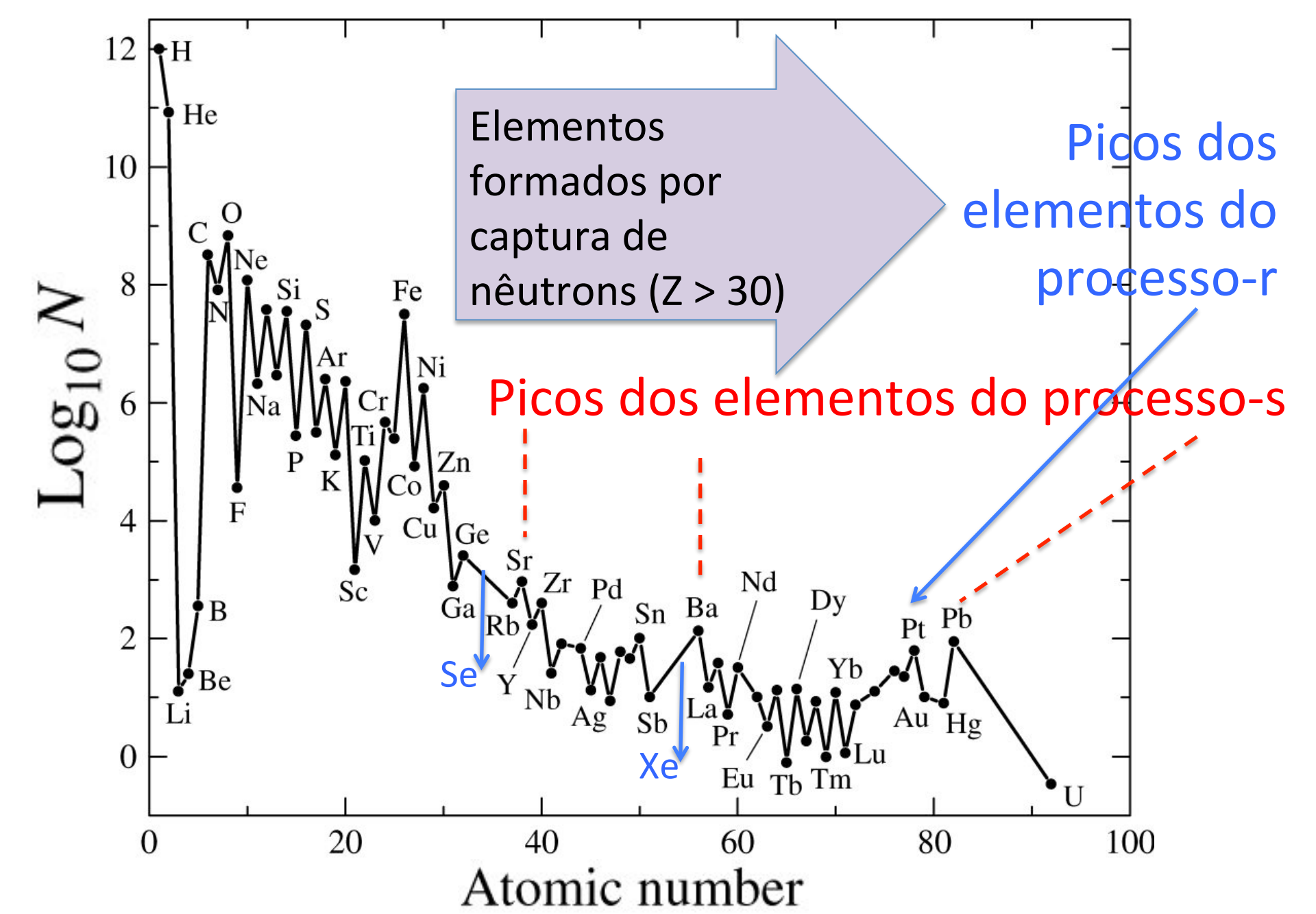

Abundância dos elementos químicos no Sol

15.4 Gamma ray bursts (GRB)

Primeiros *gamma ray bursts* detectados nos anos 1960s

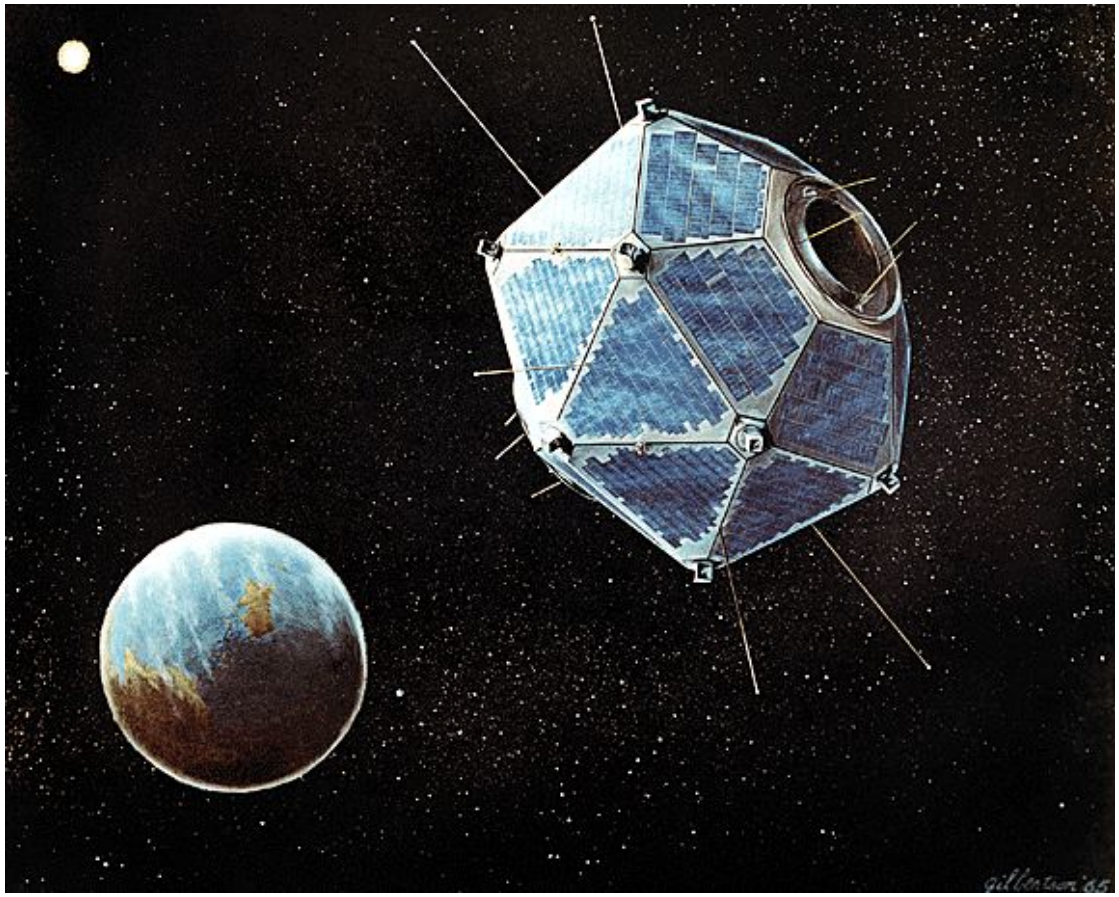

Satellite Vela that detected Gamma Ray Bursts

The Vela spacecrafts monitored the compliance of the Soviet Union to the 1963 Partial Test Ban Treaty, by looking for sudden bursts of gamma rays from nuclear weapons.

Em 1967 era clara a origem astronômica, porem GRB divulgados ao público apenas em 1973

https://en.wikibooks.org/wiki/General_Astronomy/Introduction_and_Brief_History_of_Gamma-Ray_Bursts

Gamma ray bursts

- Aproximadamente 1 por dia aleatoriamente no céu
- Energia de keV a GeV
- Duração de 10^{-2} a 10^{3} segundos
- Tempo de subida de 10^{-4} segundos, seguido de queda exponencial.
- Geralmente podem ter vários picos

Curvas de luz de 2 *Gamma ray bursts* observados pelo BATSE/Compton Gamma-Ray Observatory [CGRO]

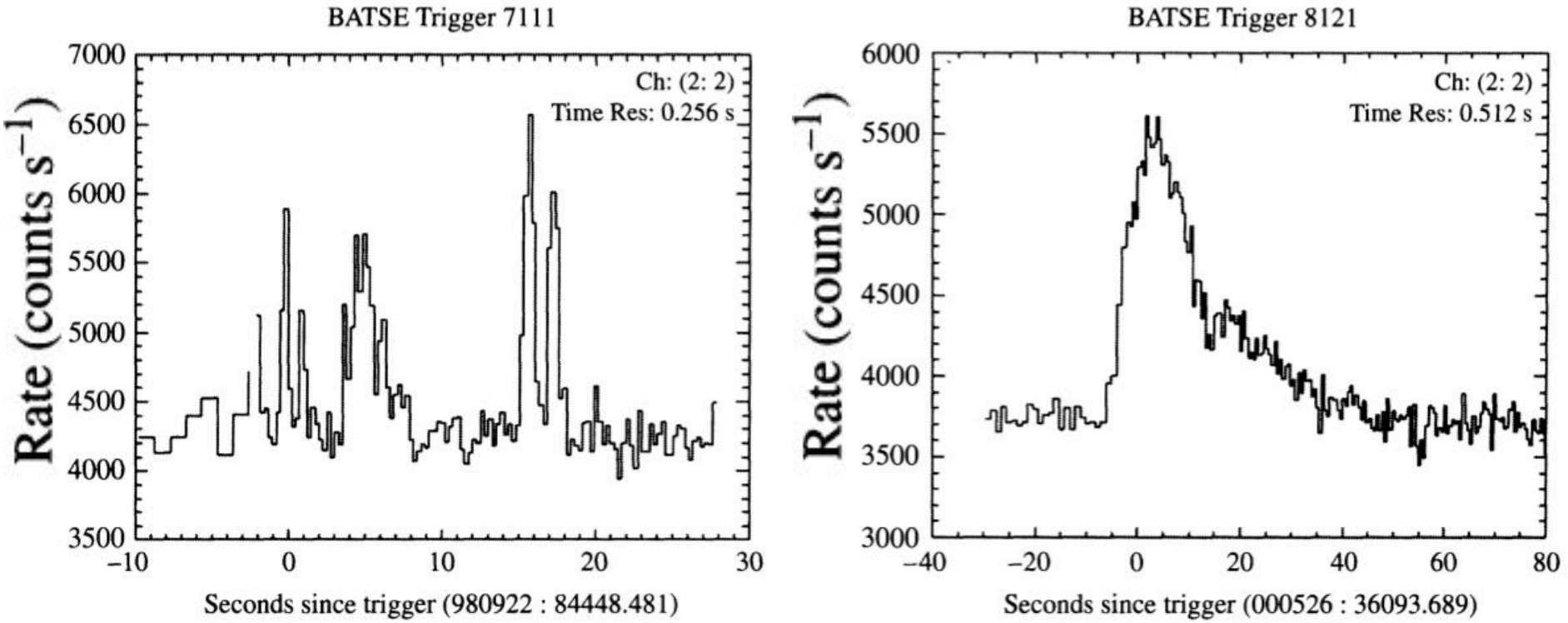

FIGURE 15.17 Light curves of two gamma-ray bursts, GRB 980922 and GRB 000526, in the energy range between 50 keV and 100 keV. The data were obtained by BATSE onboard the Compton Gamma-Ray Observatory. The dates of the two events are recorded in their designations; GRB 980922 occurred on September 22, 1998, and GRB 000526 occurred on May 26, 2000. GRB 0000526 was the last gamma-ray burst recorded by BATSE before the Compton Gamma-Ray Observatory was deorbited. (Courtesy of the BATSE Team – NASA.)

Energia liberada

Example 15.4.1. Suppose that the fluence of a particular GRB was determined to be 10^{-7} J m^{-2}. Assuming that the source of the burst was located 50,000 AU away in the Oort cloud of comets within our Solar System, and assuming further that the emission of the energy from the source was isotropic, the energy of the burst would necessarily have been

$$E = \left(4\pi r^2\right) S = 4\pi (50{,}000\ \text{AU})^2 \left(10^{-7}\ \text{J m}^{-2}\right) = 7 \times 10^{25}\ \text{J}.$$

On the other hand, if the source of the GRB were located 1 Gpc away in a distant galaxy, then the amount of energy involved in the burst (again assuming isotropy) would have been

$$E = \left(4\pi r^2\right) S = 4\pi (1\ \text{Gpc})^2 \left(10^{-7}\ \text{J m}^{-2}\right) = 1 \times 10^{45}\ \text{J},$$

comparable to the energy released in a Type II supernova, including its neutrino emission.

The difference between the two estimates is almost 20 orders of magnitude! Clearly it is critical to understand the distance to these objects in order to begin to understand the underlying process.

Distâncias desconhecidas. Proposta inicial: estrelas de nêutrons no disco espesso da nossa galáxia.

Problema: distribuição é isotrópica

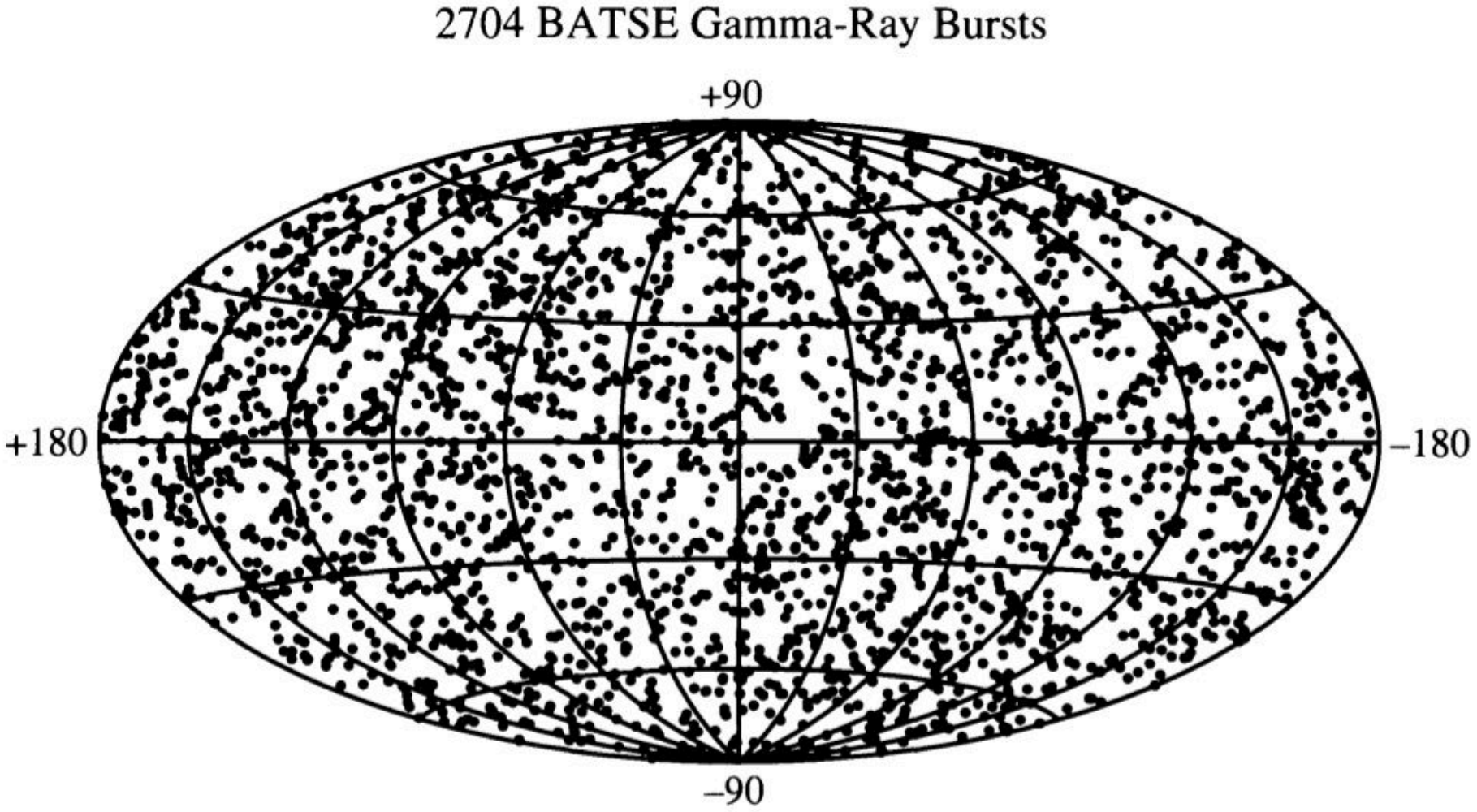

FIGURE 15.18 The isotropic angular distribution of 2704 gamma-ray bursts seen by the BATSE detector onboard the CGRO. (Courtesy of the BATSE Team – NASA.)

BeppoSAX (satélite Itália/Holanda) observou no 28 fev 1997 o GRB 970228, localizando a fonte dentro de 3 arcmin. Depois telescópios de raios-X de maior resolução localizaram melhor a fonte.

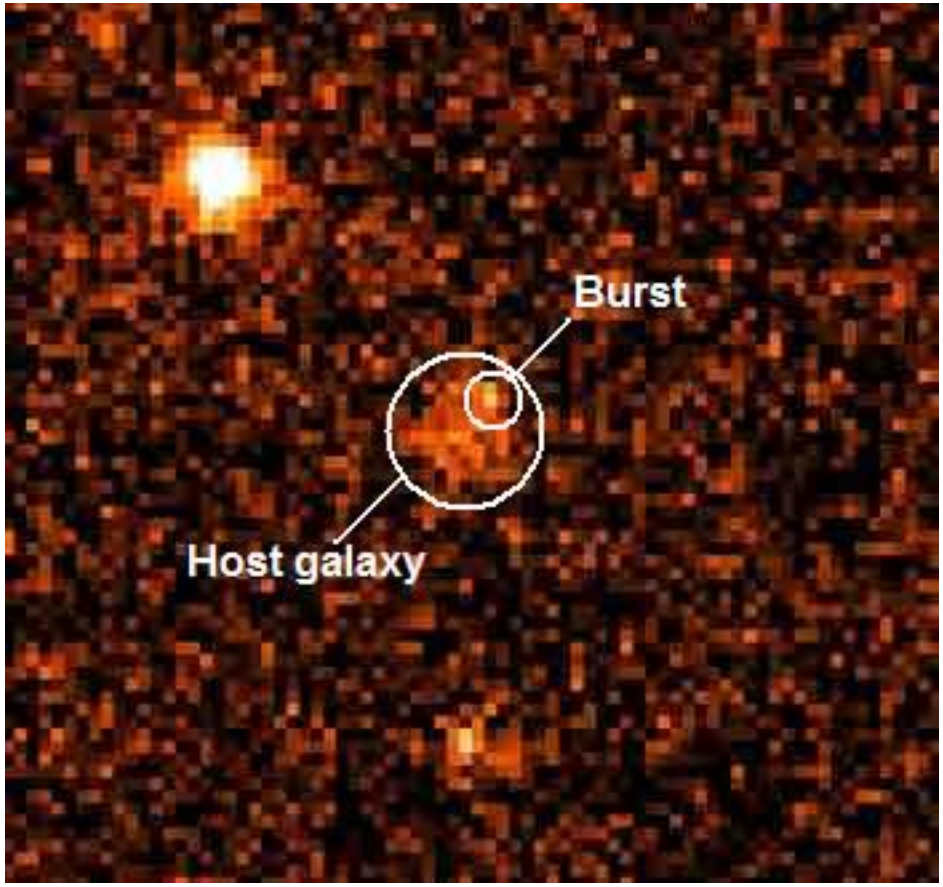

Gamma Ray Burst GRB 970228 Appears To Originate Outside Our Galaxy.

https://en.wikipedia.org/wiki/GRB_970228

Observações posteriores no óptico descobriram que a fonte está localizada em uma galáxia → origem extragaláctica dos GRBs

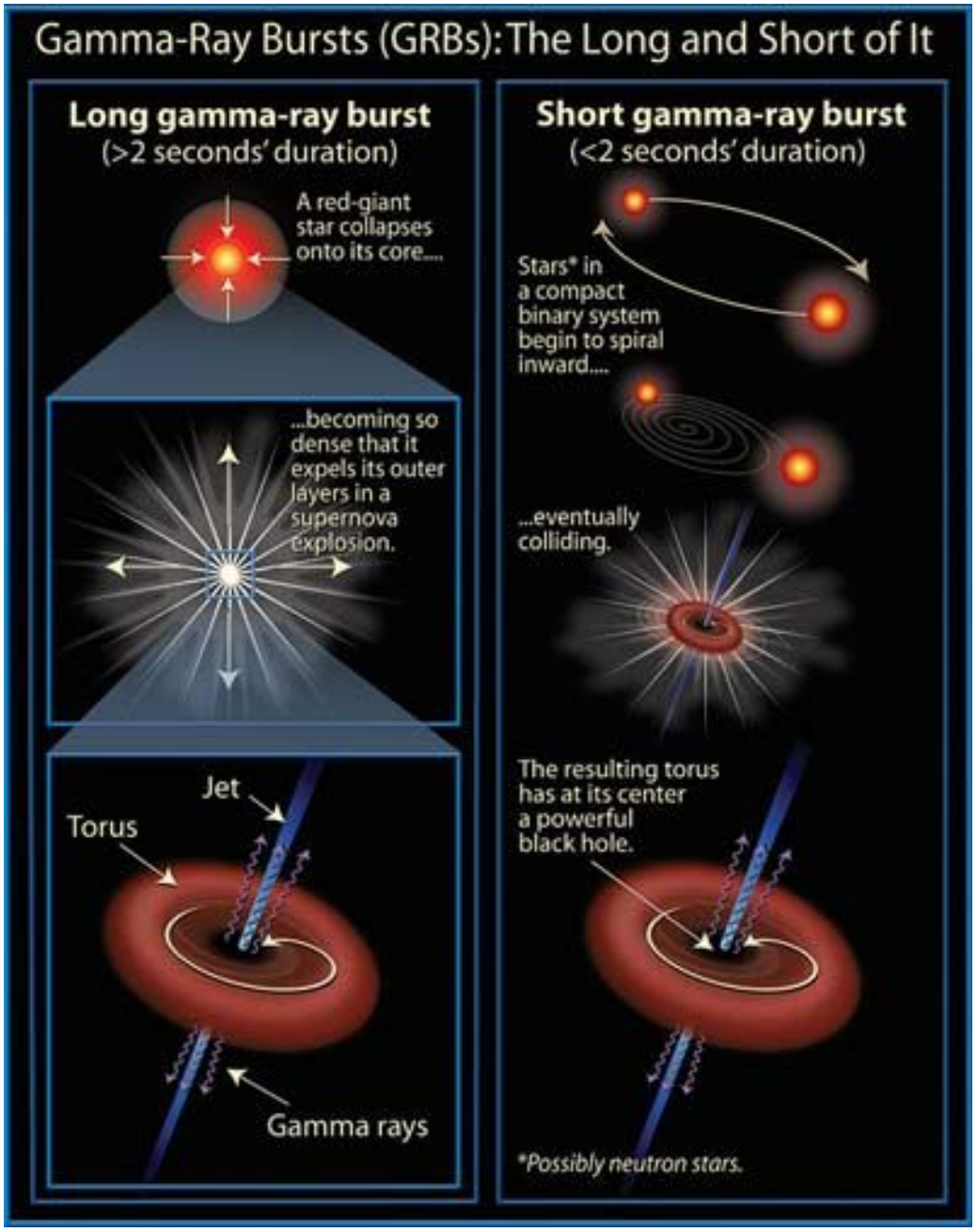

Dois tipos de GRBs.

Long-soft (> 2 segundos)
Menor energia.
Colapso e supernova.

Short-hard (< 2 segundos)
Maior energia.
Colisão de 2 estrelas de nêutrons

Conexão direta entre Long-Soft GRB e supernovas de colapso do núcleo foi bem estabelecida com o evento GRB 980425

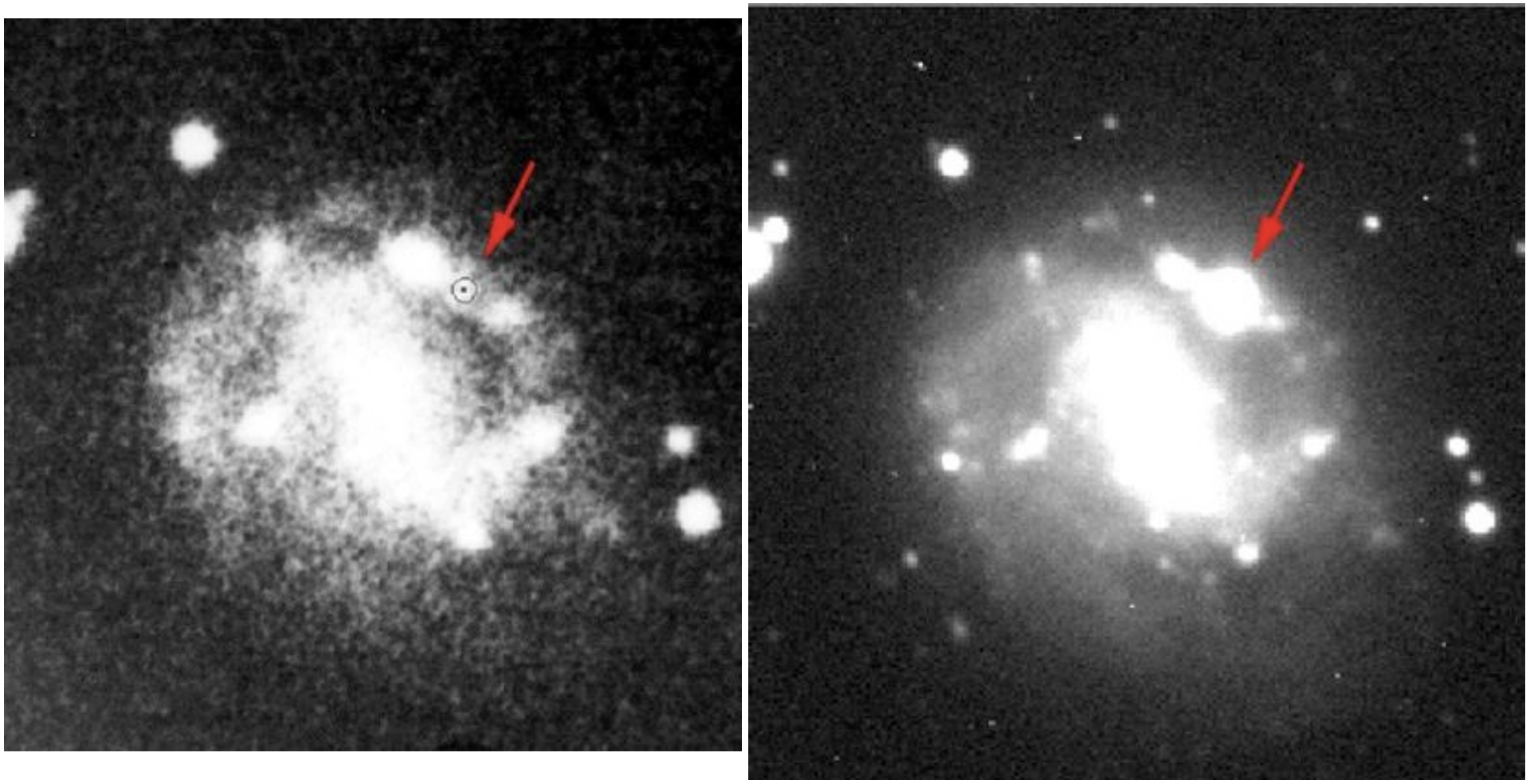

Discovery of SN 1998bw associated with GRB 980425.

GW170817 Press Release

LIGO and Virgo make first detection of gravitational waves produced by colliding neutron stars

Discovery marks first cosmic event observed in both gravitational waves and light.

Fermi

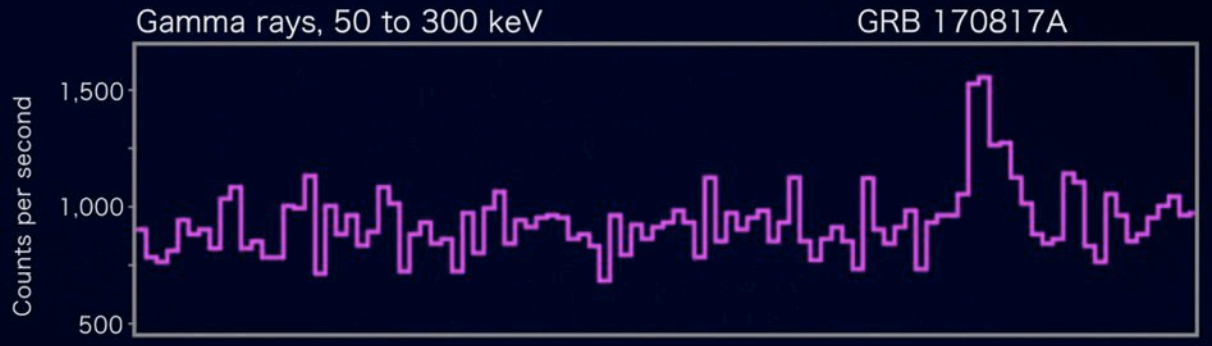

LIGO

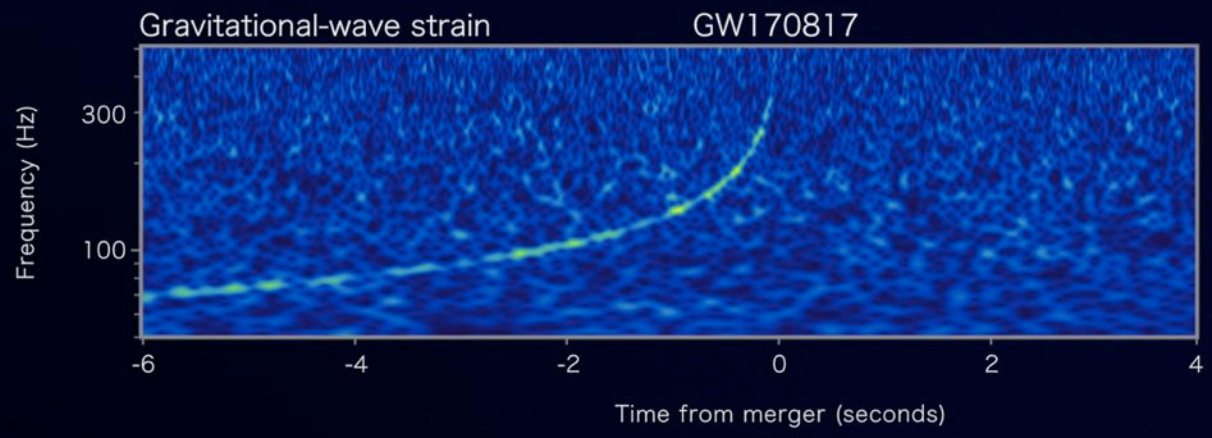

Raios-gama pela colisão de 2 estrelas de nêutrons

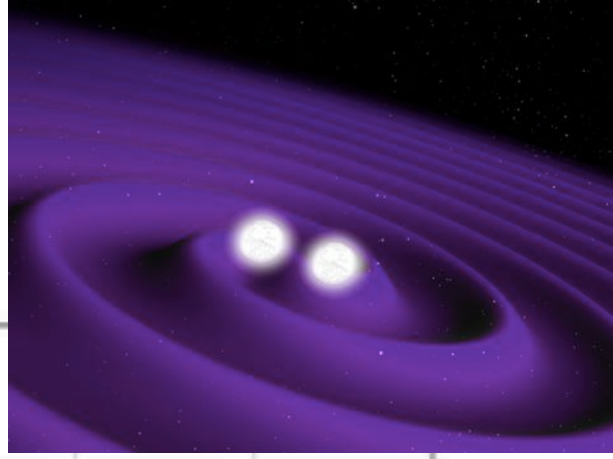

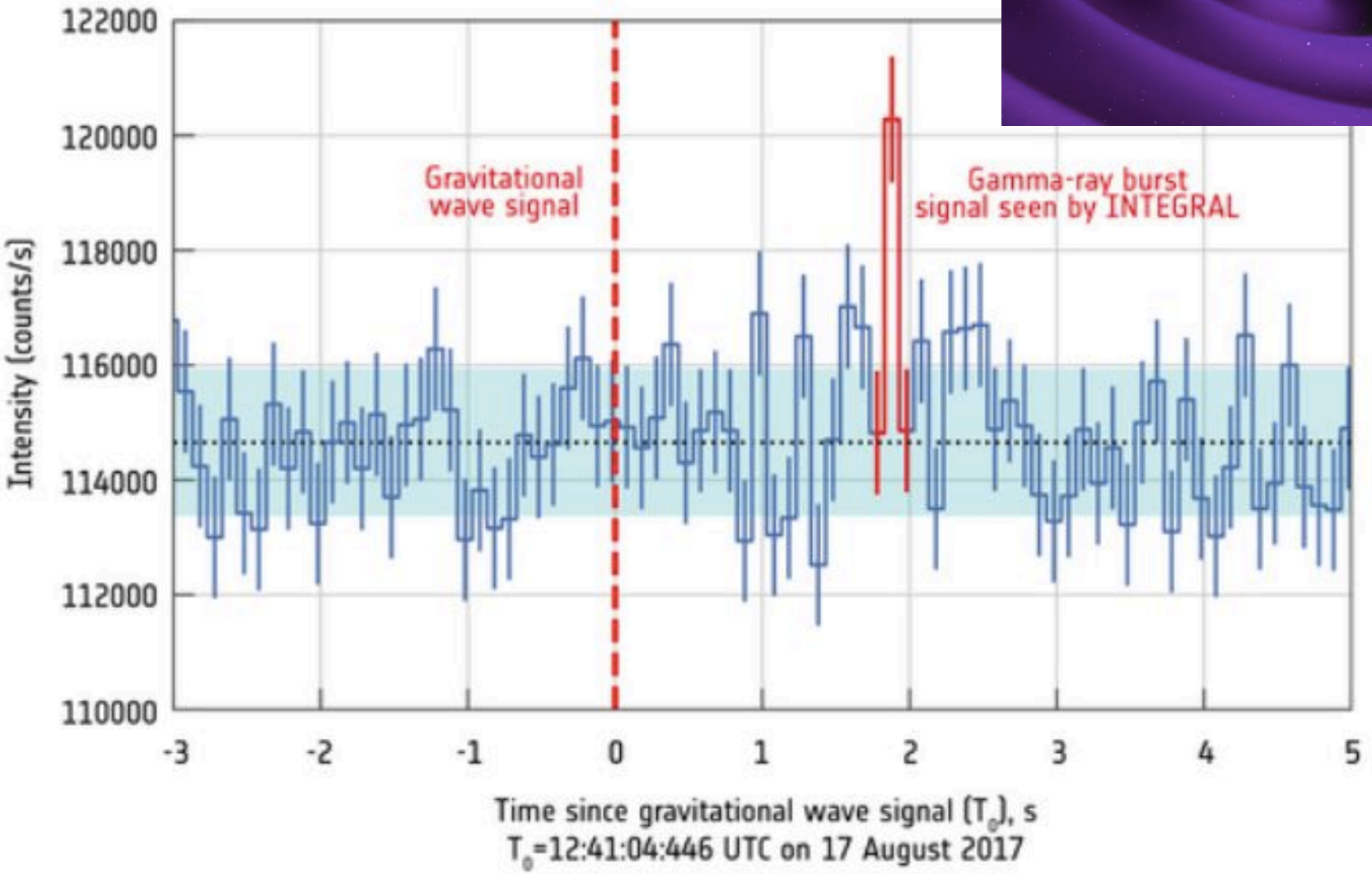

Imagem no visível da colisão de duas estrelas de nêutrons

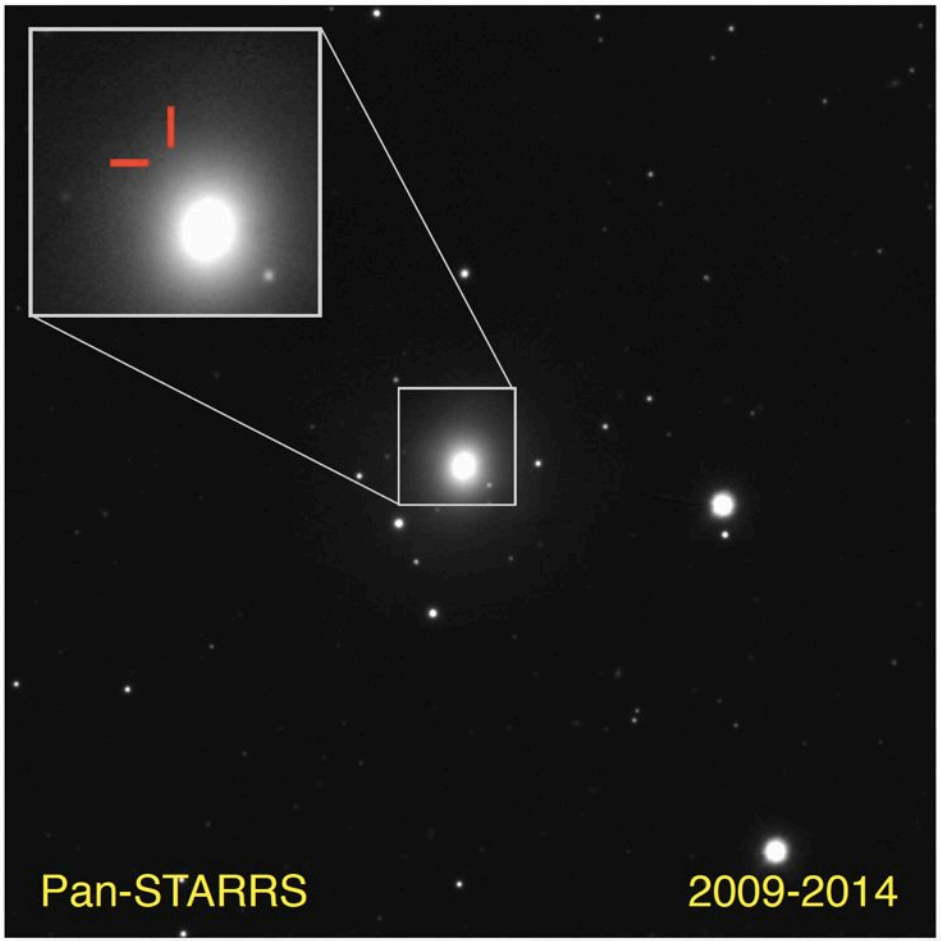

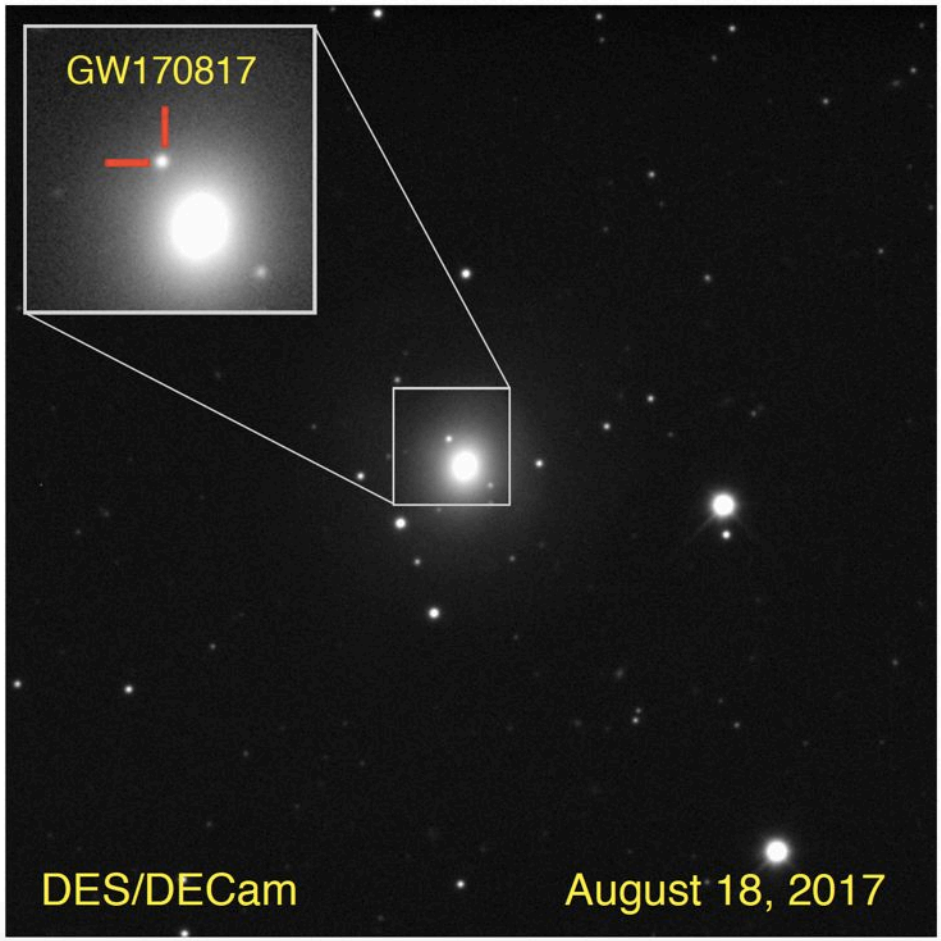

Evolução da curva de luz

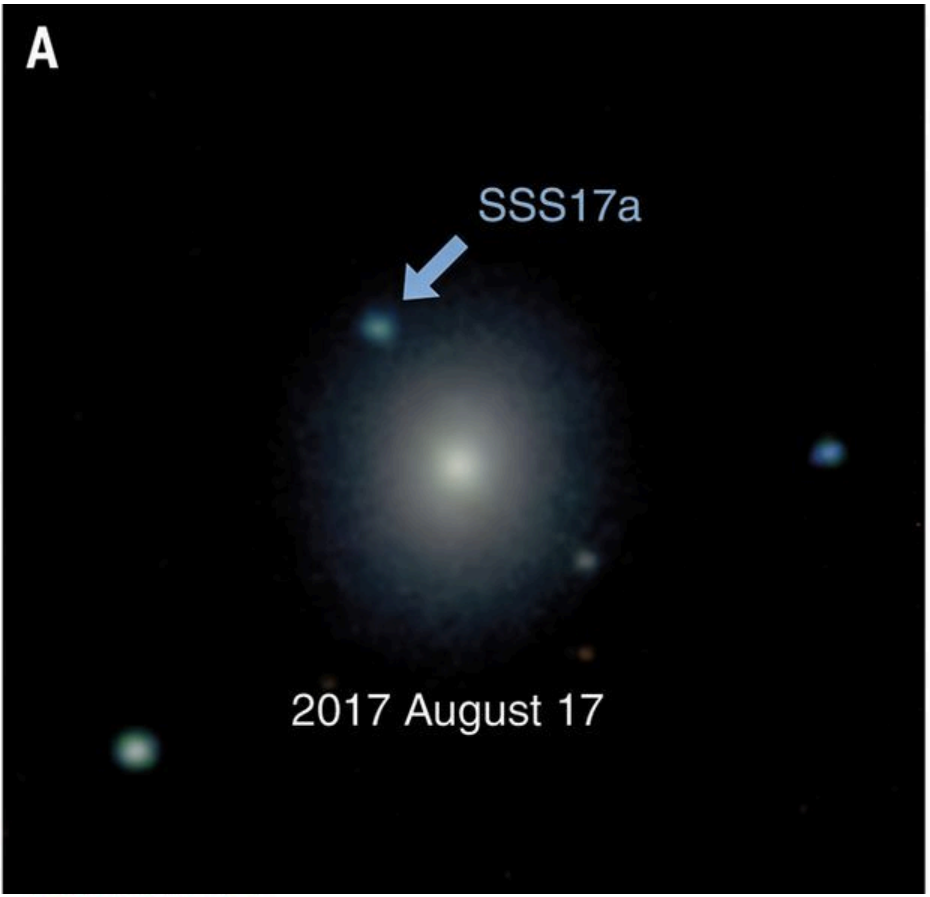

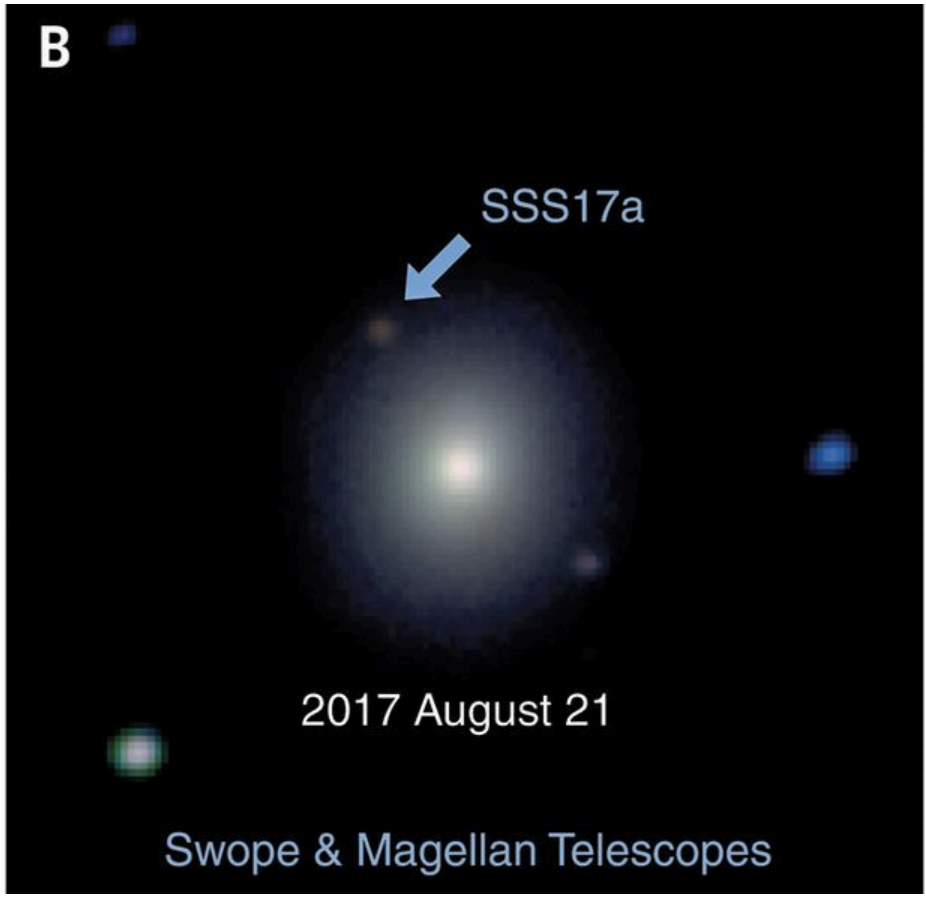

Light curves of the neutron star merger GW170817/SSS17a: Implications for r-process nucleosynthesis

M. R. Drout[1,*], A. L. Piro[1], B. J. Shappee[1,2], C. D. Kilpatrick[3], J. D. Simon[1], C. Contreras[4], D. A. Coulter[3], R. J. Foley[3], ...
+ See all authors and affiliations

Science 22 Dec 2017:
Vol. 358, Issue 6370, pp. 1570-1574

15.5 Raios cósmicos

Descobertos em 1912 por Victor Hess.

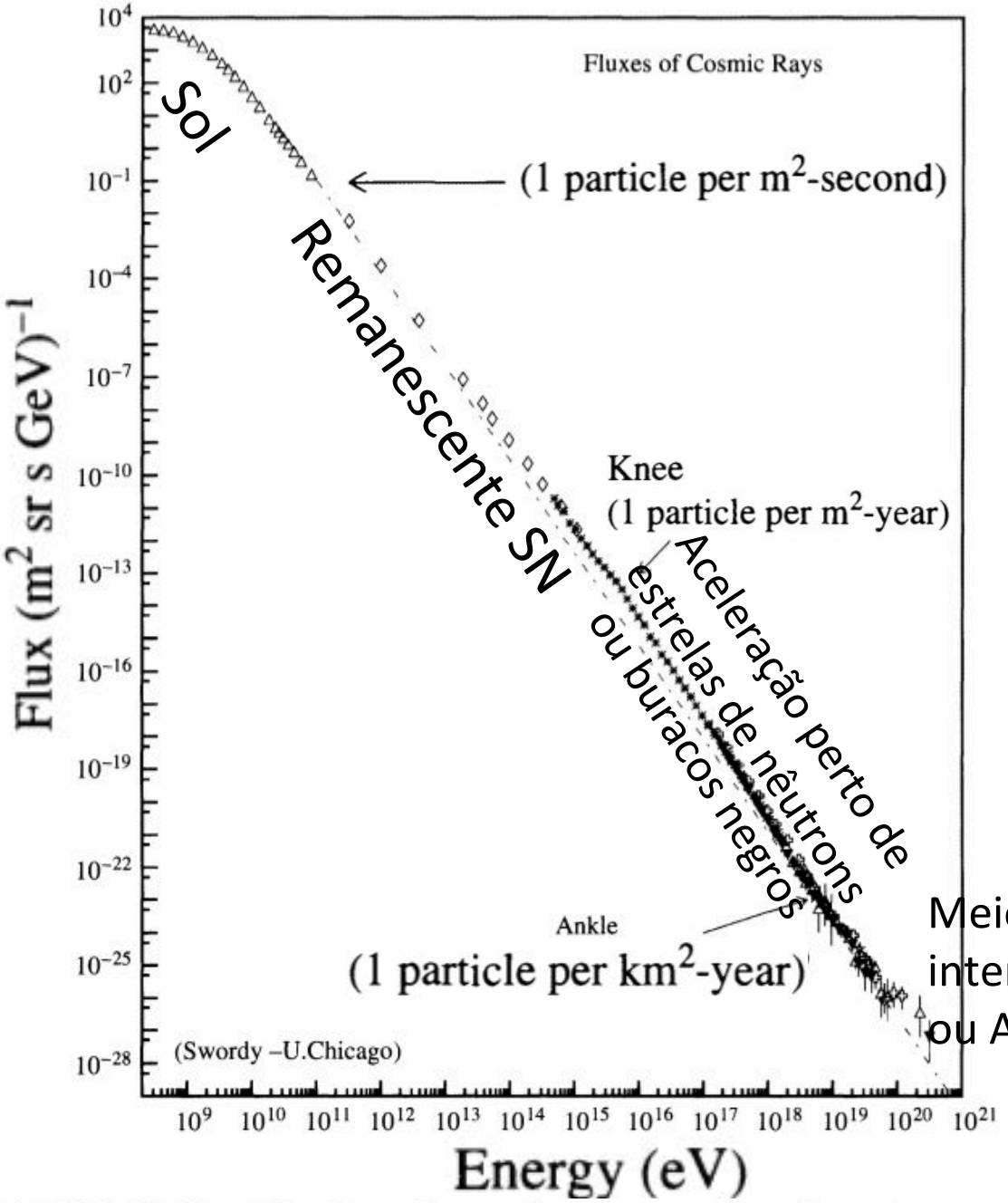

Energias:
$10^7 – 3x10^{20}$ eV

FIGURE 15.22 The flux of cosmic rays as a function of energy. (Ref: J. Cronin, T. K. Gaisser, and S. P. Swordy, *Sci. Amer.*, *276*, 44, 1997.)

15.5 Raios cósmicos. Composição

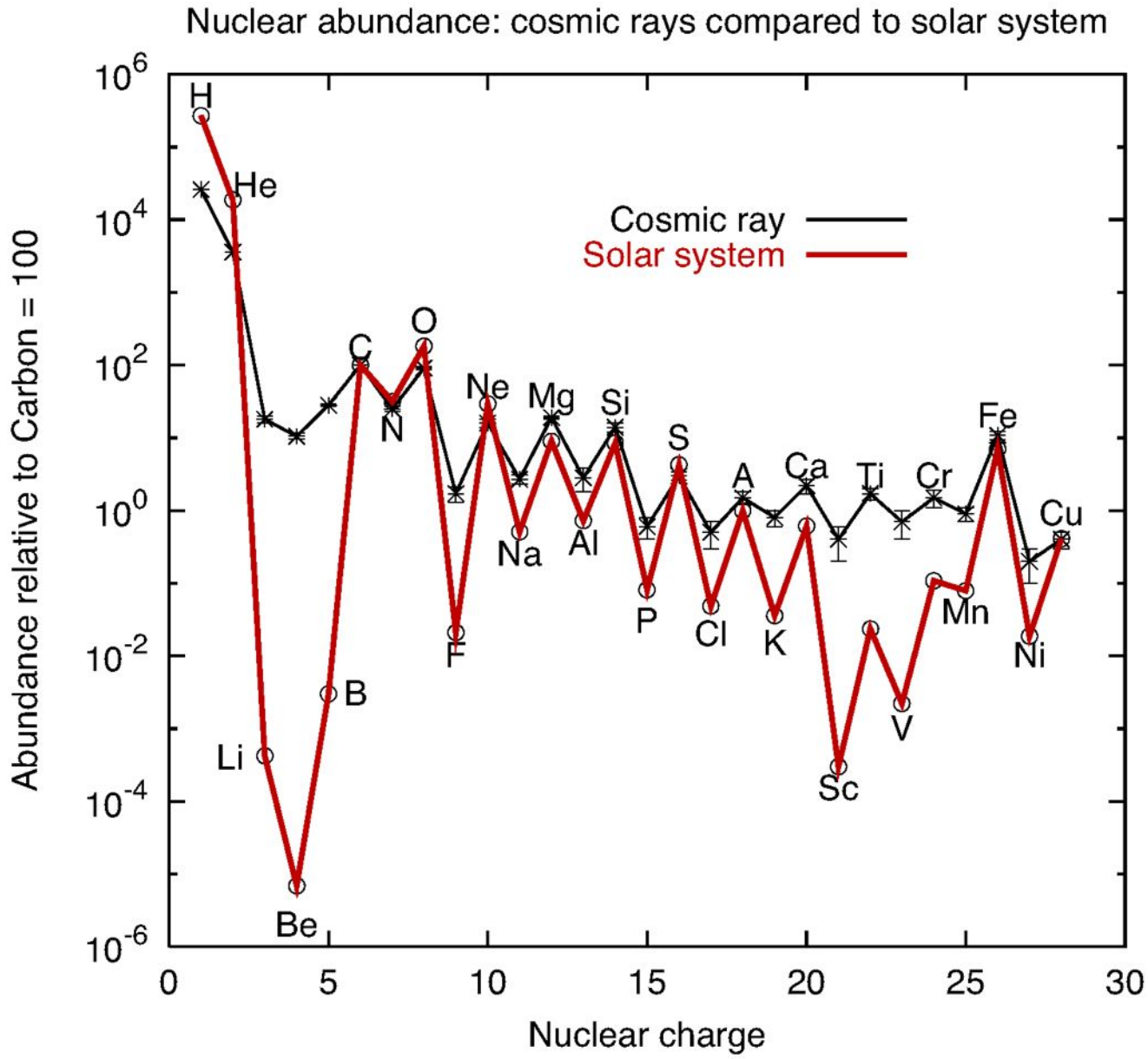

Li, Be e B podem ser produzidos no ISM devido ao processo de "*spallation*", que é a quebra de átomos de C, N e O, pelo bombardeio de raios cósmicos (p. ex., prótons)

Exemplo: *spallation* (quebra/fissão) do carbono, por por bombardeio de raio cósmico de próton

$$^{12}_{6}C + {}^{1}_{1}H \rightarrow {}^{11}_{5}B + 2\ {}^{1}_{1}H$$

$$\rightarrow {}^{10}_{5}B + {}^{3}_{2}He$$

$$\rightarrow {}^{9}_{4}Be + {}^{3}_{2}He + {}^{1}_{1}H$$

Provinha: É possível produzir Li-6 a partir de *spallation* de núcleo de ^{12}C, ^{14}N ou ^{16}O? Se sim, propor uma (1) reação

Dying low mass stars: estrelas AGB
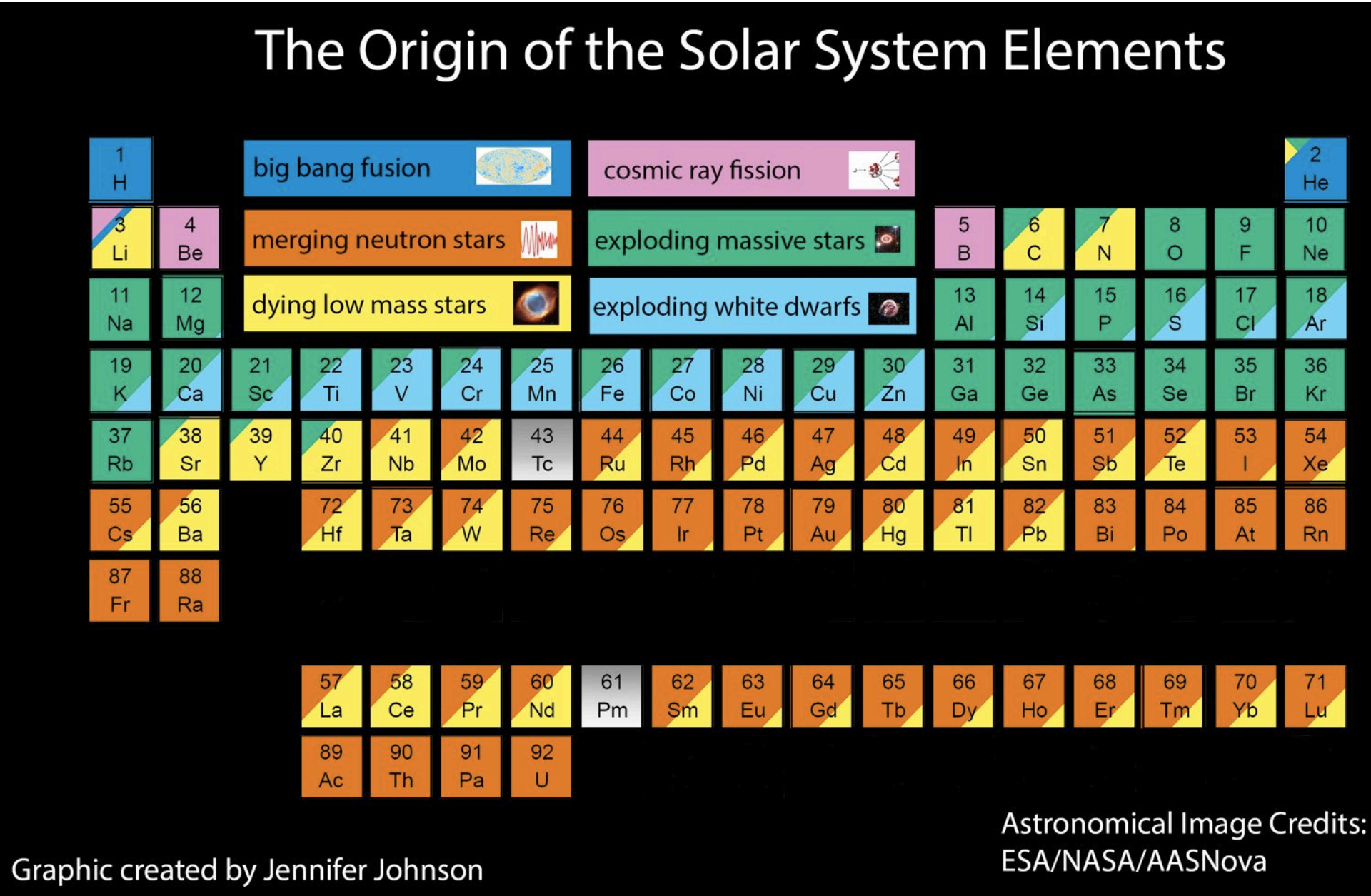
Exploding massive stars: SN type II Exploding white dwarfs: SN Ia